BAW-1794

October 1983

ANALYSIS OF CAPSULE V
Virginia Electric & Power Company
North Anna Unit No. 2

-- Reactor Vessel Materials Surveillance Program --

Babcock & Wilcox
a McDermott company

BAW-1794
October 1983

ANALYSIS OF CAPSULE V
Virginia Electric & Power Company
North Anna Unit No. 2

-- Reactor Vessel Materials Surveillance Program --

by

A. L. Lowe, Jr., PE
L. L. Collins
W. A. Pavinich
W. L. Redd
C. L. Whitmarsh

B&W Contract No. 582-7116

BABCOCK & WILCOX
Utility Power Generation Division
P. O. Box 1260
Lynchburg, Virginia 24505

CONTENTS

List of Tables

List of Figures

1. INTRODUCTION

This report describes the results of the examination of the first capsule from the Virginia Electric Power Company's North Anna Unit 2 reactor vessel surveillance program. Capsule "V" is a part of the continuing surveillance program that monitors the effects of neutron irradiation on the reactor pressure vessel materials under actual operating conditions.

The specific objectives of the program are to monitor the effects of neutron irradiation on the tensile and impact properties of the reactor pressure vessel materials under actual operating conditions and to verify the fluence calculations to which the materials are exposed. The surveillance program for the North Anna Unit 2 reactor pressure vessel materials was designed and recommended by Westinghouse Electric Company. The surveillance program and the pre-irradiation mechanical properties of the reactor vessel materials are described in WCAP-8772.[1] The surveillance program was planned to cover the 40-year design life of the reactor pressure vessel and is based on ASTM E185-73, Annex A1, "Standard Recommended Practice for Surveillance Tests for Nuclear Reactor Vessels."

This report summarizes the testing and the post-irradiation data obtained from the testing and analysis of the tensile and Charpy specimens as well as the evaluation of the thermal monitors. In addition, the dosimeters were measured and the fluence values for both the capsule materials and the reactor vessel were calculated. The wedge-opening-loading (WOL) specimens were not tested at this time, but were placed in storage to be tested later if the need for the data develops.

The future operating limitations established after the evaluation of the surveillance capsule are in accordance with the requirements of 10 CFR 50, Appendixes G and H. The recommended operating period was extended to 10 effective full-power years (EFPY) as a result of the first capsule evaluation.

2. POSTIRRADIATION TESTING

2.1. Visual Examination and Inventory

All specimens were visually examined for signs of abnormalities. The contents of the capsule were inventoried and compared with the program characterization report inventory. There was no evidence of rust or of the penetration of reactor coolant into the capsule.

The inventory of all specimens was consistent with Figure 2-6 of the Westinghouse preirradiation report.[1] However, an inconsistency was found in this report. According to Table 2-1[1], capsule V should have 8 tangential and 12 axial Charpy specimens, but Figure 2-6[1] shows 12 tangential (GT series) and 8 axial (GL series) specimens. Apparently some Charpy specimens were improperly identified. Those marked "GT" are actually axial specimens, and "GL" denotes tangential specimens. With these changes in identification, the information in Table 2-1 of the Westinghouse report is correct for the identification of capsule V material. Test data presented in the following paragraphs support this conclusion.

2.2. Thermal Monitors

Surveillance capsule V contained a temperature monitor holder block containing two fusible alloys with different melting points. The holder block was radiographed for evaluation. Neither of the two thermal monitors had melted. From these data, it was concluded that the irradiated specimens had been exposed to a maximum temperature of less than 579F during the reactor vessel operating period. This is not significantly greater than the nominal inlet temperature of 550F, and is considered acceptable. There appeared to be no significant signs of a temperature gradient along the capsule length.

2.3. Tension Testing

All tension tests were conducted in accordance with Technical Procedure LRC-TP-78 (see Appendix E); four specimens were tested. One axial base

metal specimen was tested at 550F. The weld metal specimen was damaged in a compression accident during testing and no useful data were obtained. The other weld metal and axial base metal specimens were tested at room temperature. A constant displacement rate of 0.005 in./min was imposed on each specimen until fracture. Percent total elongation, percent reduction in cross-sectional area, 0.2% offset yield strength, and ultimate tensile strength were determined in accordance with ASTM E8-69 and A370-73. These data are presented in Table 2-1.

2.4. Charpy V-Notch Impact Testing

All impact tests were conducted in accordance with Technical Procedure LRC-TP-80 (see Appendix F). The four groups of specimens (axially oriented base metal, transversely oriented base metal, weld metal, and heat-affected zone metal) were tested at temperatures between -100 and 550F. Absorbed energy, test temperature, percent shear fracture, and lateral expansion were determined in accordance with ASTM Specifications E23-73 and A370-73. Plots of test temperature versus absorbed energy, percent shear, and lateral expansion were prepared for each specimen. These data are presented in Tables 2-2 through 2-5 and Figures 2-1 through 2-4.

2.5. Material Identification

The base metal is identified in the North Anna Unit 2 reactor vessel radiation surveillance program report as Intermediate Shell Forging 04, Heat No. 990496/292424. The Intermediate Shell Forging in the FSAR is identified as Heat No. 990496/292429. It is conceivable that the difference is due to an error in transcribing the numbers (i.e., typographical error); however, because of not having the original documentation for the material the following procedure was followed. For purposes of this report, the material included in the surveillance capsule is identified by the heat number given in the surveillance program report. The heat number given in the FSAR is used to identify the material for development of pressure-temperature limits and for describing the materials used in the fabrication of the reactor pressure vessel. No effort was made to identify which of these two heat numbers is the correct one for the surveillance material.

Table 2-1. Tensile Properties of North Anna Unit 2 Capsule, V, Base and Weld Metal Irradiated to 2.41×10^{18} n/cm^2

Specimen No.	Test temp, F	Strength		Elongation, %		RA, %
		Yield, psi	Ultimate, psi	Uniform	Total	
Base Metal - Axial Orientation						
GT-4	68	85,600	104,500	7.5	18.4	45
GT-3	550	90,100	98,700	5.1	13.3	51
Weld Metal						
GW-3	68	78,600	91,600	6.2	19.7	64

Table 2-2. Charpy Impact Data for North Anna Unit 2, Capsule V, Base Metal, Tangential Orientation, Irradiated to 2.41×10^{18} n/cm^2

Specimen No.	Test temp, F	Absorbed energy, ft-lb	Lateral expansion, mils	Shear fracture, %
GL-10	-40.	24.0	18.0	0.
GL-12	0.	31.0	26.0	5.
GL-15	20.	47.0	36.0	10.
GL-9	68.	69.0	51.0	30.
GL-14	220.	121.0	94.0	100.
GL-13	330.	95.0	74.0	100.
GL-11	440.	107.5	67.0	100.
GL-16	550.	102.5	81.0	100.

Table 2-3. Charpy Impact Data for North Anna Unit 2, Capsule V, Base Metal, Axial Orientation, Irradiated to 2.41×10^{18} n/cm^2

Specimen No.	Test temp, F	Absorbed energy, ft-lb	Laterial expansion, mils	Shear fracture, %
GT-19	-100.	1.5	2.0	0.
GT-14	-40.	5.0	6.0	0.
GT-18	20.	11.0	11.0	5.
GT-21	49.	23.0	66.0	10.
GT-13	68.	31.0	26.0	5.
GT-15	98.	50.0	43.0	30.
GT-16	123.	37.0	36.0	20.
GT-17	162.	43.0	43.0	30.
GT-24	220.	58.0	60.0	100.
GT-23	330.	63.0	56.0	100.
GT-22	440.	58.0	60.0	100.
GT-20	550.	60.0	61.0	100.

Table 2-4. Charpy Impact Data for North Anna Unit 2, Capsule V, Base Metal, Heat-Affected Zone, Irradiated to 2.41×10^{18} n/cm^2

Specimen No.	Test temp, F	Absorbed energy, ft-lb	Laterial expansion, mils	Shear fracture, %
GH-14	-100.	3.0	5.0	5.
GH-18	-40.	32.0	28.0	20.
GH-24	0.	64.0	41.0	50.
GH-20	20.	68.0	48.0	60.
GH-16	40.	62.0	49.0	10.
GH-19	68.	50.0	44.0	50.
GH-23	98.	100.0	97.0	100.
GH-17	118.	88.0	66.0	100.
GH-22	220.	87.0	60.0	100.
GH-21	330.	84.0	56.0	100.
GH-15	440.	79.0	73.0	100.
GH-13	550.	71.0	63.0	100.

Table 2-5. Charpy Impact Data For North Anna Unit 2, Capsule V, Weld Metal, Irradiated to 2.41×10^{18} n/cm^2

Specimen No.	Test temp, F	Absorbed energy, ft-lb	Laterial expansion, mils	Shear fracture, %
GW-19	-100.	2.0	7.0	5.
GW-16	-40.	16.5	18.0	20.
GW-18	-12.	29.0	40.0	20.
GW-21	0.	48.5	47.0	40.
GW-17	20.	58.0	51.0	50.
GW-14	20.	63.5	53.0	40.
GW-23	68.	74.0	62.0	100.
GW-24	121.	92.0	73.0	70.
GW-20	220.	92.0	83.0	100.
GW-15	330.	102.5	84.0	100.
GW-22	440.	105.0	85.0	100.
GW-13	550.	103.0	91.0	100.

Figure 2-1. Charpy Impact Data From Irradiated Base Metal, Tangential Orientation

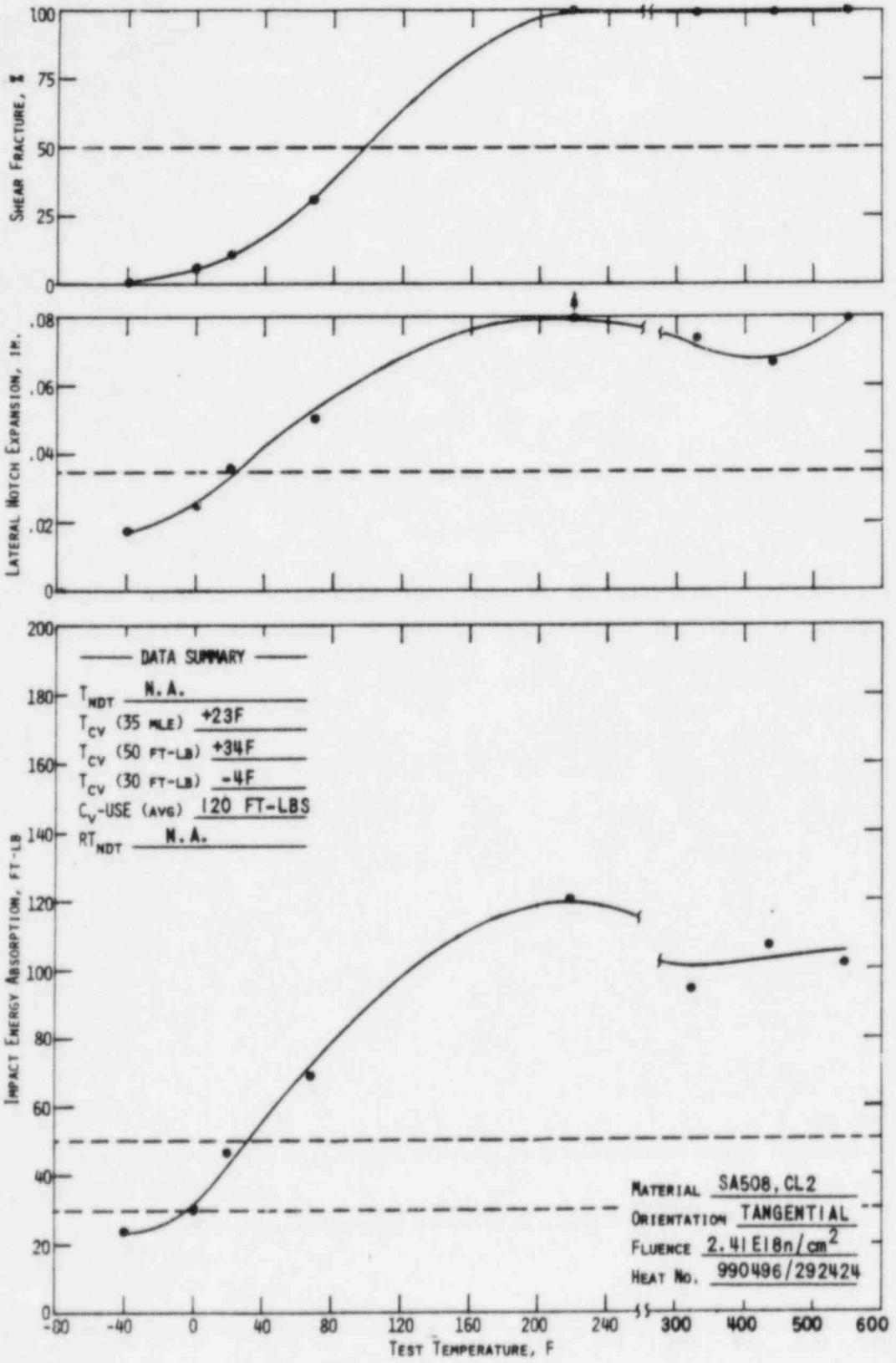

Figure 2-2. Charpy Impact Data From Irradiated Base Metal, Axial Orientation

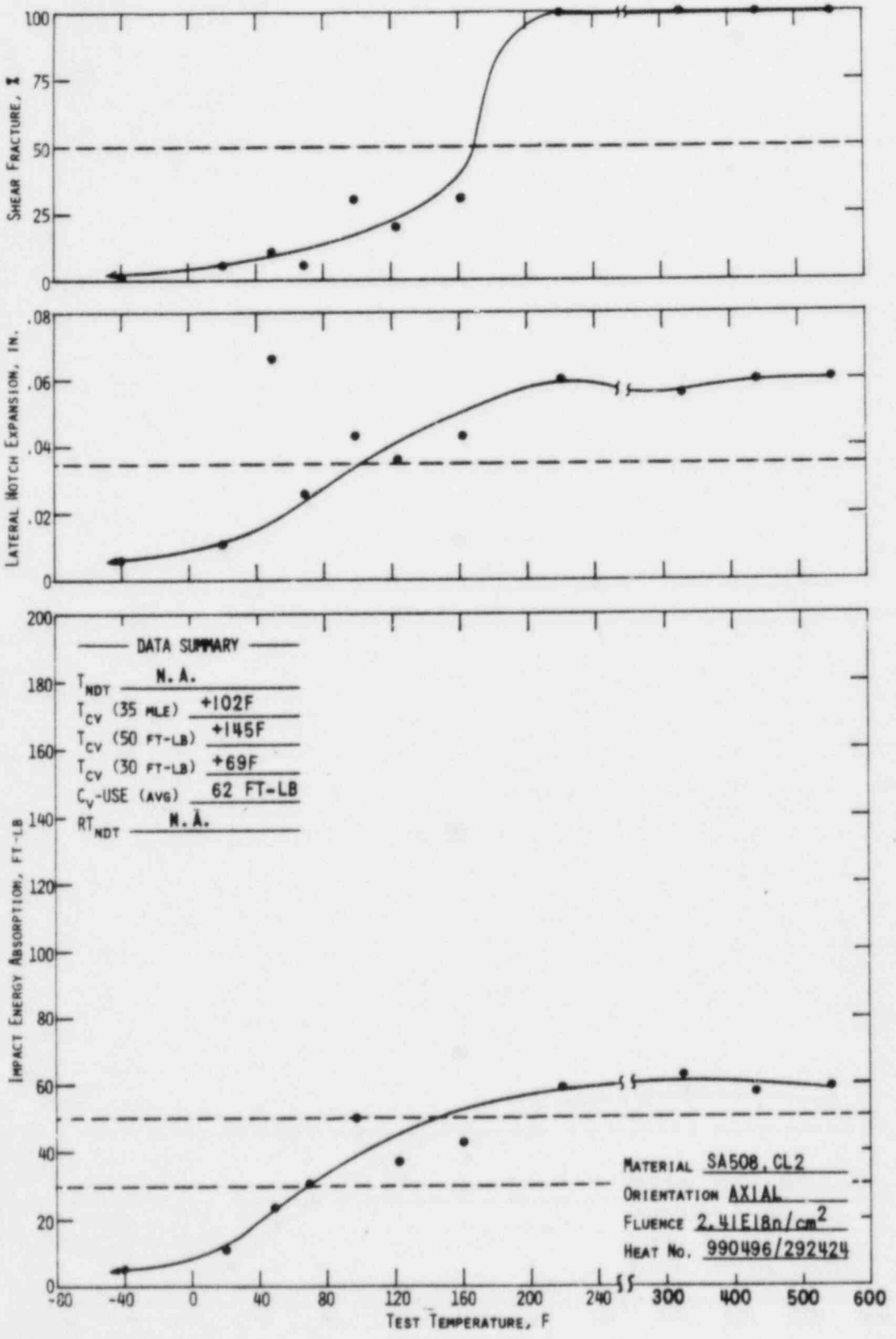

Figure 2-3. Charpy Impact Data From Irradiated Base Metal, Heat-Affected Zone

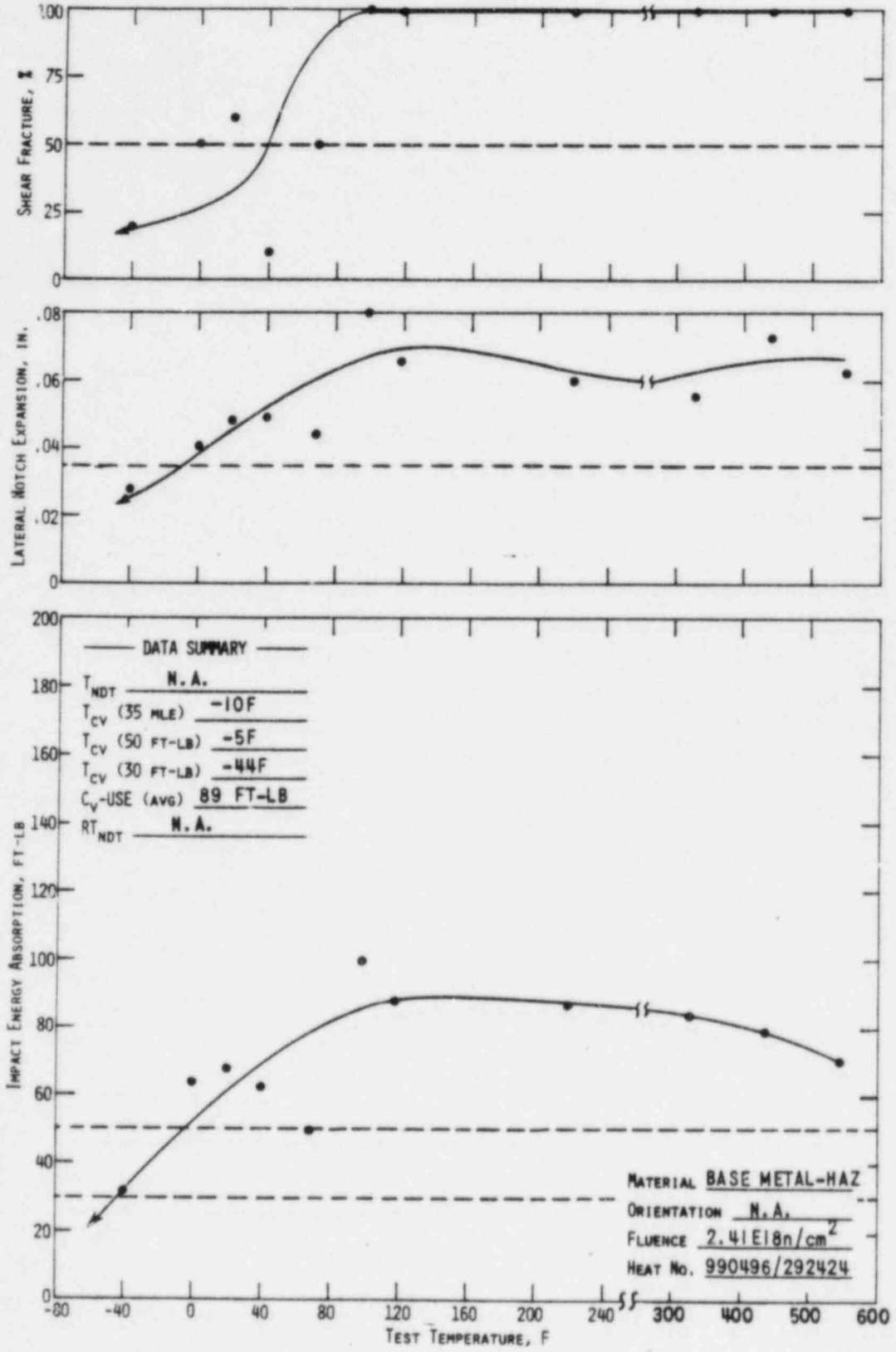

Figure 2-4. Charpy Impact Data From Irradiated Weld Metal

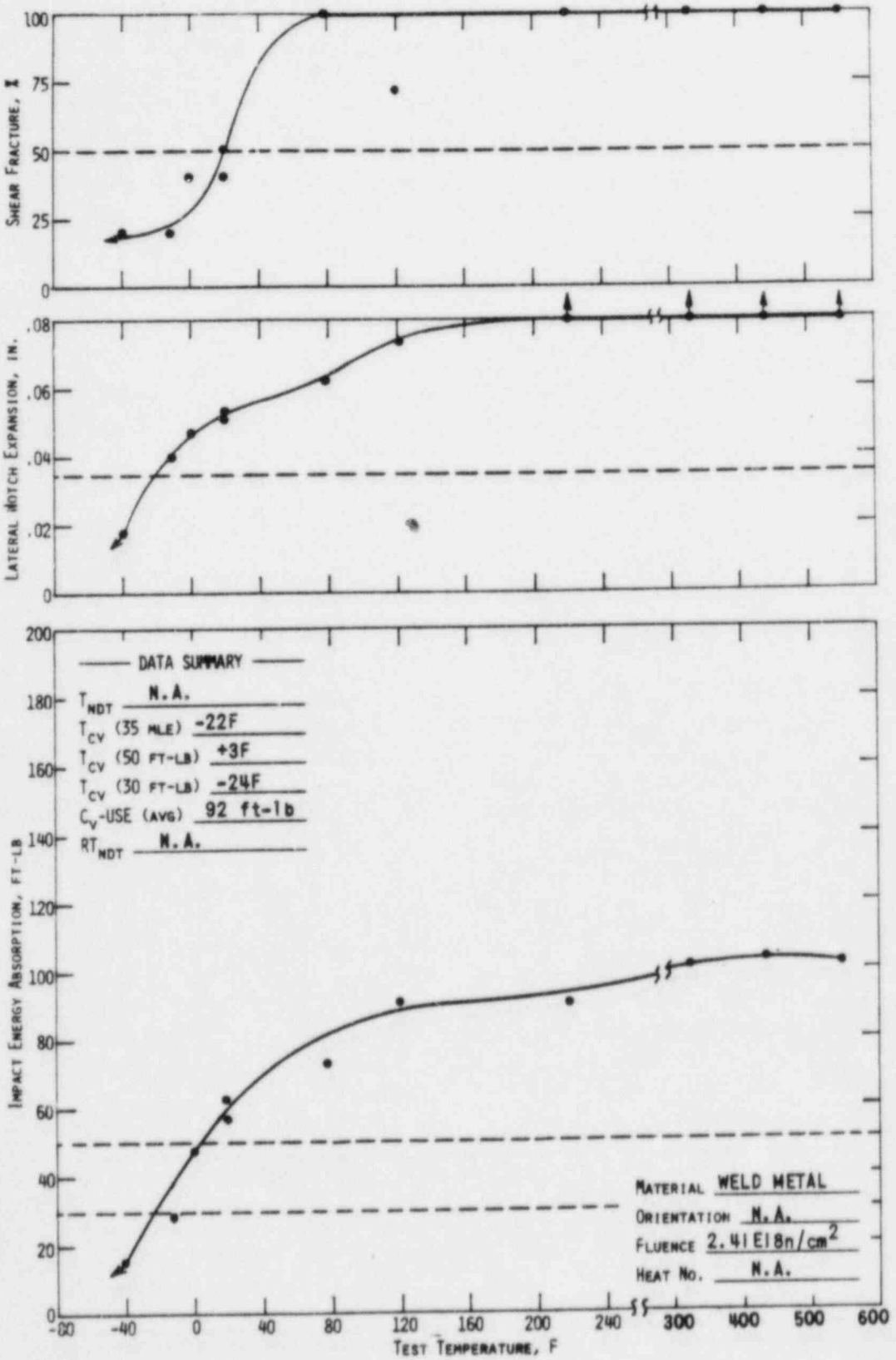

3. NEUTRON DOSIMETRY

3.1. Introduction

Fluence data are required to (1) provide a correlation between radiation-induced property changes and fluence for surveillance specimens, (2) determine exposure of the pressure vessel at the maximum flux location, and (3) predict long-term exposure of the pressure vessel at the location of maximum flux and at weld locations. Fluence to the surveillance specimens is measured with passive dosimeters that are included in each capsule. The corresponding reactions in these detectors are listed in Table 3-1.

Because of a long half-life of 30 years and an effective energy range of >0.5 MeV, the measurements of ^{137}Cs production from fission reactions in ^{237}Np and ^{238}U are most applicable for analytical determinations of fast (E > 1MeV) fluence during cycle 1. The other dosimeter reactions are useful as corroborating data for shorter time intervals and/or higher energy fluxes. Short-lived isotope activities are representative of reactor conditions only over the latter portion of the irradiation period (full cycle); whereas reactions with threshold energy >2 or 3 MeV do not record a sufficient fraction of the total fast flux.

The energy-dependent neutron flux is not directly available from activation detectors because the dosimeters record only the integrated effect of the neutron flux on the target material as a function of both irradiation time and neutron energy. To obtain an accurate estimate of the time-averaged neutron flux incident upon the detector, the following parameters must be known: the operating history of the reactor, the energy response of the given detector, and the neutron spectrum at the detector location. Of these parameters, the definition of the neutron spectrum is the most difficult to obtain. Essentially, two means are available to obtain the spectrum: iterative unfolding of experimental data and analytical methods. Due to a lack

of sufficient threshold detectors satisfying both the threshold energy and half-life requirements necessary for a surveillance program, calculated spectra are used to convert activity to flux and fluence.

The approach used in this analysis is to calculate fast flux distributions in the capsule and the reactor vessel regions. These calculated fluxes are normalized at the capsule by comparison of measured to calculated dosimeter activities. This normalization factor is applied to all calculated fluxes in the capsule and the vessel. Fluence is obtained by a time integration of flux over the capsule irradiation period. Long-term fluence predictions are made by adjusting flux for future fuel cycle effects and then integrating over the time period of interest. This procedure is summarized in Figure 3-1.

3.2. Analytical Model

Energy-dependent neutron fluxes at the detector locations were determined by a discrete ordinates solution of the Boltzmann transport equation with the two-dimensional code, DOT 3.5.[2] The North Anna Unit 2 reactor was modeled from the core to the shield tank in R-Theta geometry (based on a plan view along the core midplane and one-eighth core symmetry in the azimuthal dimension; see Figure 3-2 and Table 3-2). Also included was an explicit model of a surveillance capsule at the proper location (shown schematically in Figure 3-3). The center of Capsule V was positioned 191.69 cm (75.47 inches) from the core center and 15.0° off axis. The reactor model contained the following nine regions: core, liner, bypass coolant, core barrel, inlet coolant, thermal shield, pressure vessel, cavity, and shield tank. Input parameters to the code included a pin-by-pin time-averaged power distribution, CASK23E 22-group microscopic neutron cross sections[3], S_8 order of angular quadrature, and P_3 expansion of the scattering cross-section matrix.

Because of computer storage limitations, it was necessary to use two geometric models to cover the distance from the core to the primary shield. A boundary source output from the initial model A (core into the pressure vessel) was used to "bootstrap" a model B, which included the capsule.

Flux output from the DOT 3.5 calculations in R-θ geometry required an axial distribution adjustment to account for axial effects. Thus, fluxes were multiplied by an axial shape factor to correlate capsule elevation and axial flux distribution. Capsule V extended about 50 inches above and below the core midplane. The axial factor ranged from 1.06 to 1.19 for various dosimeter locations in the capsule and was 1.20 at the maximum location in the pressure vessel.

The calculation described above provides the neutron flux as a function of energy at the detector position. These calculated data are used in the following equations to obtain the calculated activities used for comparison with the experimental values. The basic equation for the activity D (in μCi/gm) is given as follows:

$$D_i = \frac{Nf_i}{A_i\ 3.7\times10^4} \sum_E \sigma_n(E)\phi(E) \sum_j F_j \quad (1 - e^{-\lambda_i t_j})_e^{-\lambda_i T_f} \qquad (6\text{-}1)$$

where

N = Avogadro's number,

A_i = atomic weight of target material i,

f_i = either weight fraction of target isotope in nth material or fission yield of desired isotope,

$\sigma_n(E)$ = group-averaged cross sections for material n, listed in Table D-3,

$\phi(E)$ = group-averaged fluxes calculated by DOT analysis,

F_j = fraction of full power during jth time interval, t_j,

λ_i = decay constant of ith material,

t_j = time interval of reactor operation,

T_f = decay time from end of jth interval.

$$C = \frac{D\ (\text{measured})}{D(\text{calculated})} \qquad (6\text{-}2)$$

where D(calculated) is obtained from equation 6-1.

Measured activity is determined for each dosimeter using established ASTM procedures. Counting rates, which are obtained with a multichannel Ge(Li) gamma spectrometer, are converted to specific activity at the time of removal from the reactor. Calculated activity is also referenced to reactor shutdown, as indicated in equation 6-1, with power history data (fractional full power versus calendar time).

All calculated fluxes are then normalized as follows:

$$\phi = C\ \phi\ (\text{calculated}). \qquad (6\text{-}3)$$

3.3. Results

Calculated activities are compared to dosimeter measurements in Table 3-3. The fission wire data indicate about a 6% underprediction of fast flux (E > 1 MeV) by the analytical model described herein; non-fission wire data were overpredicted by 4 to 16%. As noted previously, non-fission wire results are used only to corroborate fission wire data. Fission wire data were also corroborated with additional fission product reactions not reported here. A value of 1.06 was selected for the normalization factor and then applied to all calculated fluxes. Thus, fast flux (E > 1 MeV) was determined to be 7.40 (+10) n/cm^2-s in the capsule (center dosimeter location at core midplane) and 5.67 (+10) n/cm^2-s at the pressure vessel maximum location (Table 3-4). Corresponding fluence values for cycle 1 (376.4 EFPD at 2775 Mw) were 2.41 (+18) n/cm^2 and 1.84 (+18) n/cm^2, respectively. Flux exposures for E > 0.1 MeV were greater by more than a factor of 2.5. The maximum location in the pressure vessel was at the inside surface along a major axis (across flats diameter) and about 80 cm below core midplane. The capsule lead factor (ratio of fast flux in the capsule to maximum fast flux in the pressure vessel) was 1.31 based on a central location of Charpy specimens. To convert to the capsule center, multiply all capsule fluxes and fluences by 1.058.

In order to translate dosimeter measurements to calculations and to specimen locations, it is necessary to know flux gradients inside of the capsule. Sufficient details are included in the calculational model to show a radial gradient of about 20% between front and back Charpy specimens and an

azimuthal gradient of about 5% between side-by-side specimens (Figure 3-4). Effects of the axial position can be seen in Figure 3-5. Thus, midplane values that are listed in Table 3-4 can be converted to other locations within a capsule by a radial factor (Figure 3-4) and a ratio of axial factors, local to midplane (Figure 3-5).

Flux spectra were calculated in the capsule, at the vessel surface, and at two locations in the vessel, 1/4T and 1/2T. The data listed in Table 3-5 indicate that, relative to the capsule, the flux energy spectrum is somewhat harder (higher average energy) at the vessel surface, quite similar at 1/4T, and softer (lower average energy) at 1/2T. These spectra imply that when E > 1 MeV fluence is used to correlate material damage, capsule specimens represent metal near the vessel 1/4T position. Because of different spectral shapes at other locations, E > 1 MeV flux correlations may be less accurate. Also of note is the significant fraction of E > 1 MeV flux at energies < 2.5 MeV, an energy range where the $^{54}Fe(n,p)$ and $^{58}Ni(n,p)$ reactions have little response (Table D-2). Dosimeter reaction cross sections, averaged over the capsule spectrum, are listed in Table 3-6. The corresponding fast flux that was derived from the measured activities shows a range of values with the two fission reactions at the higher end, copper at the lower end, and the nickel and iron reactions near mid-range. This same trend has been observed in previous analyses. As noted previously, analytical results were normalized to the fission reactions. Also included in Table 3-6 is the thermal flux of 7.5 (+10) n/cm^2-s in the capsule that was derived from bare and Cd-covered cobalt dosimeters. This value is sufficiently low so that measured reaction rates in the non-shielded dosimeters are not affected.

Cycle 1 fluence was extrapolated to the 32 EFPY vessel design life by assuming proportionality to fast flux escaping the core from fuel management criticality analyses of cycles 2 and 3. Cycle 3, which utilized once-burned fuel on the core periphery, was assumed to be representative of an equilibrium cycle. This procedure accounts for the changes in relative power distribution resulting from fuel shuffling between fuel cycles and effectively translates cycle 1 results to equilibrium cycle results. Lifetime fluences (32 EFPY) at several pressure vessel locations are listed in Table 3-7, and as noted above are based on a low-leakage fuel cycle design. Fluence as a function of penetration through the pressure vessel is shown in Figure 3-6.

To facilitate estimation of flux (and/or fluence) at other capsule locations, the azimuthal variation of fast flux is plotted in Figure 3-7. Although the data were calculated at the vessel surface, they should be applicable at the capsule radius also. Since all other capsule locations are situated at angles >15° off axis, the corresponding lead factors will be less than the capsule V lead factor.

Uncertainties were estimated for the fluence values reported herein. These data, listed in Table 3-8, were based on comparisons to benchmark experiments when available, estimated and measured variations in input data, and engineering judgment. Because of the complexity of fluence calculations for reactor vessel surveillance, no comprehensive uncertainty limits exist for these results. The values in Table 3-8 represent a best-estimate based on considerable experience in this type of analysis.

Table 3-1. Surveillance Capsule Detectors

Detector reaction	Energy range, Mev	Isotope half-life
$^{54}Fe(n,p)^{54}Mn$	>2.5	313 days
$^{58}Ni(n,p)^{58}Co$	>2.3	71.2 days
$^{63}Cu(n,\alpha)^{60}Co$	>5.0	5.27 years
$^{238}U(n,f)^{137}Cs$	>1.1	30.1 years
$^{237}Np(n,f)^{137}Cs$	>0.5	30.1 years

Table 3-2. Calculation Model for North Anna Unit 2

Component	Material	Outer radius, cm[a]
Core	Homogenized mixture of UO_2, coolant, cladding, structure	161.32
Core liner	SS304	164.18
Bypass coolant	Water (583F, 2250 psia, 500 ppm B)	170.02
Core barrel	SS304	175.10
Inlet coolant	Water (547F, 2250 psia, 500 ppm B)	181.13
Thermal shield	SS304	187.96
Inlet coolant[b]	Water (547F, 2250 psia, 500 ppm B)	199.39
Pressure vessel[c]	SA508	219.29
Cavity	Air (130F, 15 psia)	236.22
Shield tank	SA508	237.49
Shield[d]	Water (70F, 15 psia)	245.00

(a)Measured along a major axis (across core flats diameter).

(b)Capsule is in this region.

(c)Dimension includes 40 cm liner on inner surface.

(d)Model was attenuated; partial dimension only.

Table 3-3. Dosimeter Activations

Reaction	A Measured activity, μCi/g	B Calculated activity, μCi/g	C=A/B Normalization Constant
$^{54}Fe(n,p)^{54}Mn$	835(a)	893(b)	0.93
$^{58}Ni(n,p)^{58}Co$	1583(a)	1650(b)	0.96
$^{63}Cu(n,\alpha)^{60}Co$	1.97	2.28	0.86
$^{238}U(n,f)^{137}Cs$	2.86	2.73	1.05
$^{237}Np(n,f)^{137}Cs$	20.6	19.3	1.07

(a)Average of dosimeter wires from Table D-2.

(b)Average of dosimeter locations in calculational model.

Table 3-4. Neutron Flux and Fluence(a)

	E > 1 MeV		E > 0.1 MeV	
	Fast flux n/cm^2-s	Fast fluence for cycle 1, n/cm^2 (376.4 EFPD)	Flux n/cm^2-s	Fluence for cycle 1, n/cm^2 (376.4 EFPD)
Capsule, central dosimeter location(b)	7.40 (+10)	2.41 (+18)	2.04 (+11)	6.63 (+18)
Pressure vessel	5.67 (+10)	1.84 (+18)	1.45 (+11)	4.72 (+18)

(a)Estimated uncertainties are ±16% at the capsule and ±24% at the vessel surface.

(b)Approximate geometric center of the Charpy specimens at core midplane; to convert to geometric center of the capsule, multiply by 1.058.

Table 3-5. Calculated Neutron Flux Spectra

Group Flux Normalized to E > 1 MeV[a]

Energy range, MeV	Capsule center	Vessel Surface	Vessel 1/4T	Vessel 1/2T
12.2-15	6.9 (-4)	1.04(-3)	8.7 (-4)	7.9 (-4)
10.0-12.2	2.99(-3)	4.24(-3)	3.50(-3)	3.12(-3)
8.18-10.0	8.40(-3)	1.14(-2)	9.06(-3)	7.71(-3)
6.36-8.18	2.24(-2)	2.90(-2)	2.18(-2)	1.72(-2)
4.96-6.36	4.33(-2)	5.32(-2)	4.02(-2)	3.13(-2)
4.06-4.96	4.25(-2)	5.09(-2)	3.71(-2)	2.80(-2)
3.01-4.06	7.65(-2)	8.42(-2)	6.50(-2)	5.17(-2)
2.46-3.01	9.16(-2)	9.68(-2)	8.09(-2)	6.73(-2)
2.35-2.46	3.00(-2)	3.20(-2)	2.73(-2)	2.29(-2)
1.83-2.35	1.55(-1)	1.58(-1)	1.52(-1)	1.40(-1)
1.11-1.83	4.22(-1)	3.89(-1)	4.32(-1)	4.54(-1)
1.0 -1.11	1.06(-1)	9.17(-2)	1.32(-1)	1.78(-1)

(a) $\phi_g = \frac{\text{flux in energy group g}}{\text{flux with E > 1 MeV}}$.

Table 3-6. Dosimetry Results

Reaction	Microscopic cross section $\bar{\sigma}$, b/atom[a]	Derived fast flux E ≥ 1 Mev n/cm^2-s[b]
$^{54}Fe(n,p)^{54}Mn$	0.0831[c]	6.53 (+10)
$^{58}Ni(n,p)^{58}Co$	0.111[c]	6.71 (+(10)
$^{63}Cu(n,\alpha)^{60}Co$	9.26(-4)[c]	6.05 (+10)
$^{238}U(n,f)^{137}Cs$	0.386	7.31 (+10)
$^{237}Np(n,f)^{137}Cs$	2.61	7.43 (+10)
$^{59}Co(n,\gamma)^{60}Co$	37	7.5 (+10)[d]

(a) $$\bar{\sigma} = \frac{\int_0^\infty \sigma(E)\,\phi(E)\,dE}{\int_1^\infty \phi(E)\,dE}.$$

(b) Values are referenced to geometric center of Charpy specimens.

(c) Average values for multiple dosimeters.

(d) Thermal flux derived from bare and Cd-covered cobalt dosimeters.

Table 3-7. Predicted Lifetime Fluence (32 EFPY) to Pressure Vessel for E > 1 MeV[a]

	Vessel surface[b]	1/4T	3/4T
Average fast flux, n/cm^2-s[c]	4.9 (+10)	2.9 (+10)	6.9 (+9)
Fast fluence, n/cm^2	4.9 (+19)	2.9 (+19)	6.9 (+18)

(a) At an elevation about 80 cm below core midplane and on a major axis (across flats core diameter).

(b) Estimated uncertainty of ±28% for maximum value at vessel surface.

(c) $\bar{\phi} = \dfrac{\int_0^t \phi(t)dt}{t} = \dfrac{\text{fluence}}{\text{time}}$

Table 3-8. Estimated Fluence Uncertainty

Result	Estimated uncertainty	Input parameters
1. Fast fluence in the capsule.	±16%	Activity measurement. Conversion from activity to fluence.
2. Fast fluence in the vessel, maximum flux location, capsule irradiation time interval.	±24%	Item 1 Location of oxide powder. Location of capsule. Radial flux extrapolation. Azimuthal flux extrapolation. Capsule perturbation of flux.
3. Fast fluence in the vessel, maximum flux location, end of life.	±28%	Item 2 Time extrapolation from capsule irradiation to 32 EFPY.

Figure 3-1. Flowchart for Fluence Analysis

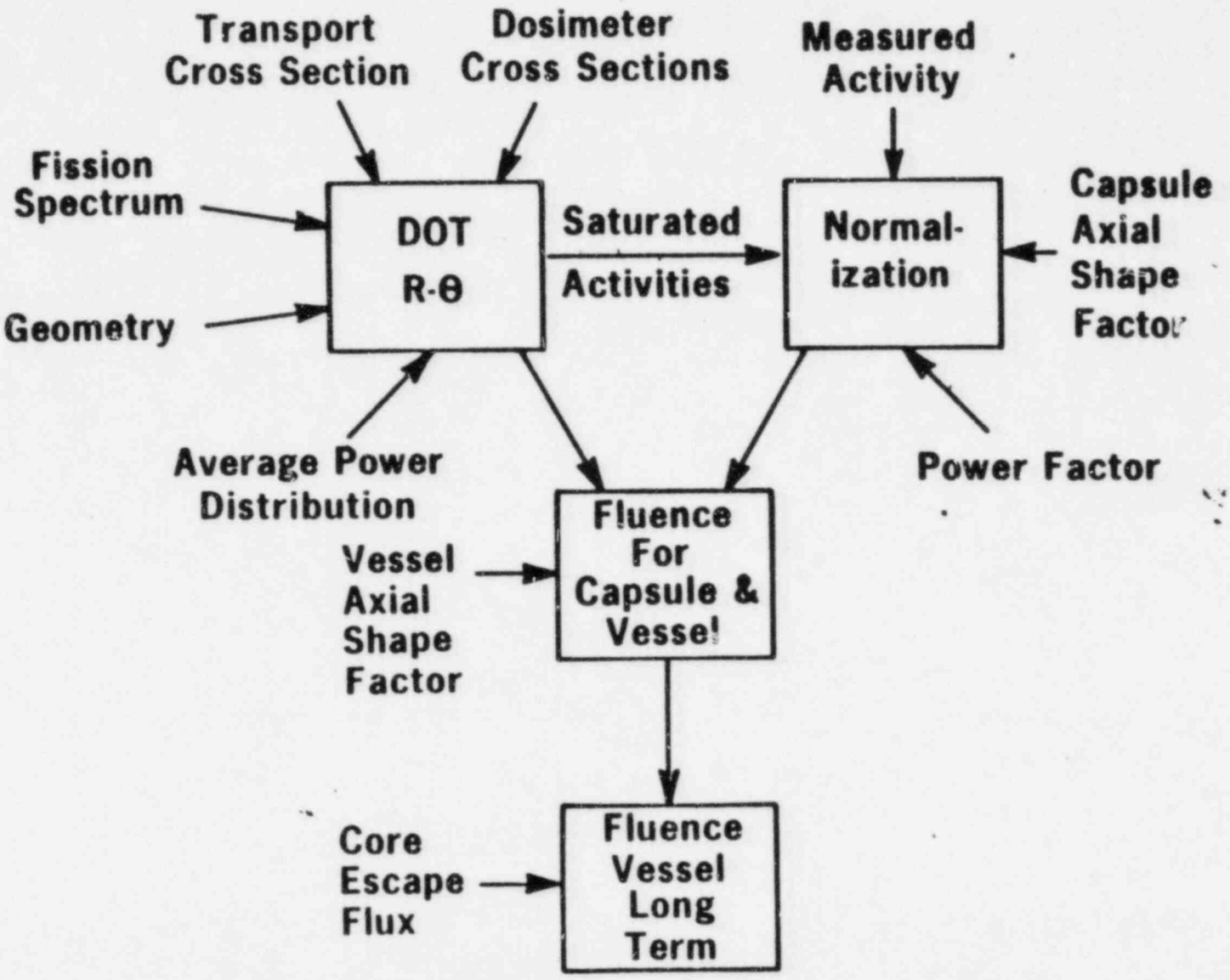

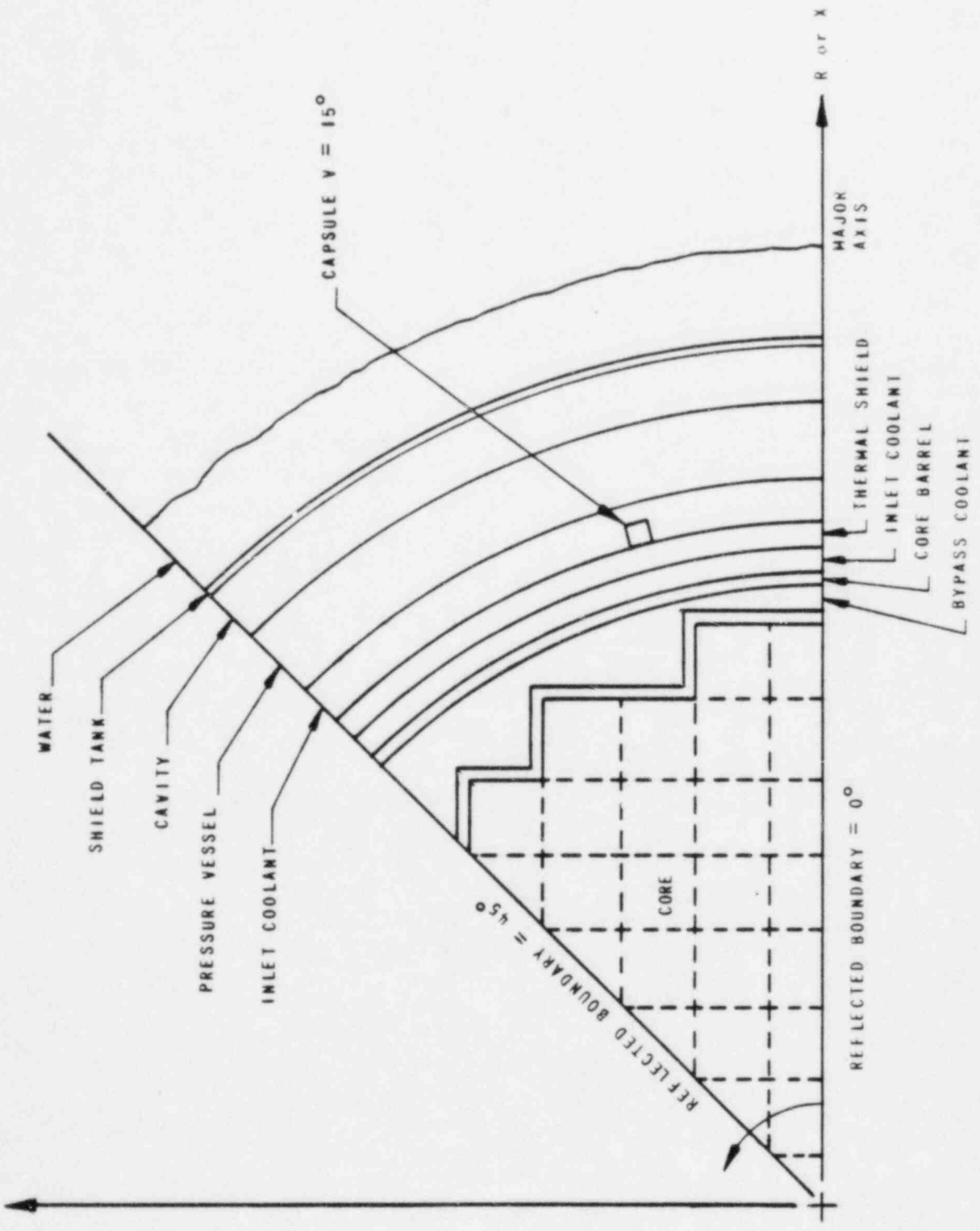

Figure 3-2. Calculation Model of the North Anna Unit 2 Reactor

Figure 3-3. Surveillance of Capsule Geometry in North Anna Unit 2

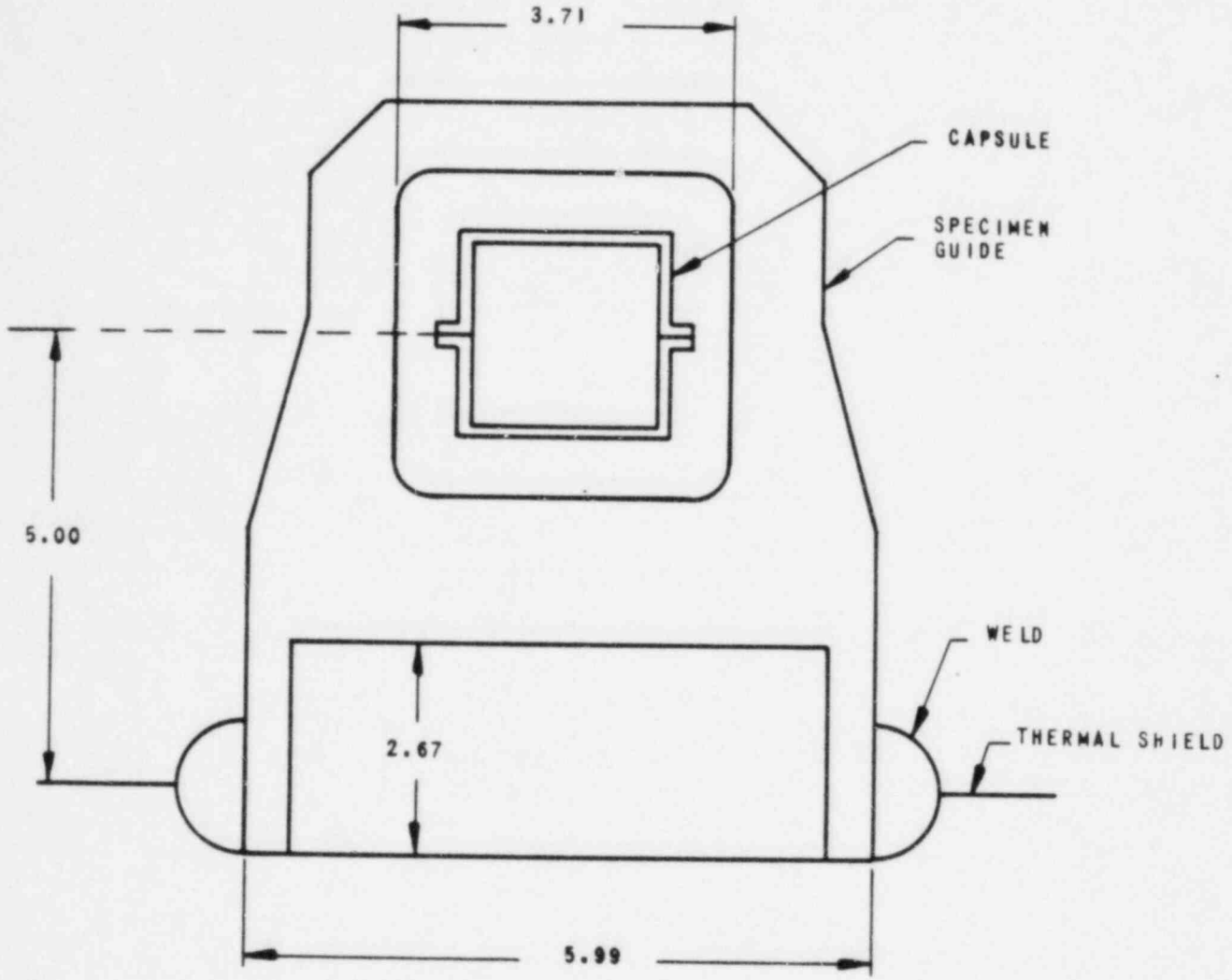

NOTE: ALL DIMENSIONS ARE CM

Figure 3-4. Relative Fast Flux at Specimen and Dosimeter Locations in Surveillance Capsule V

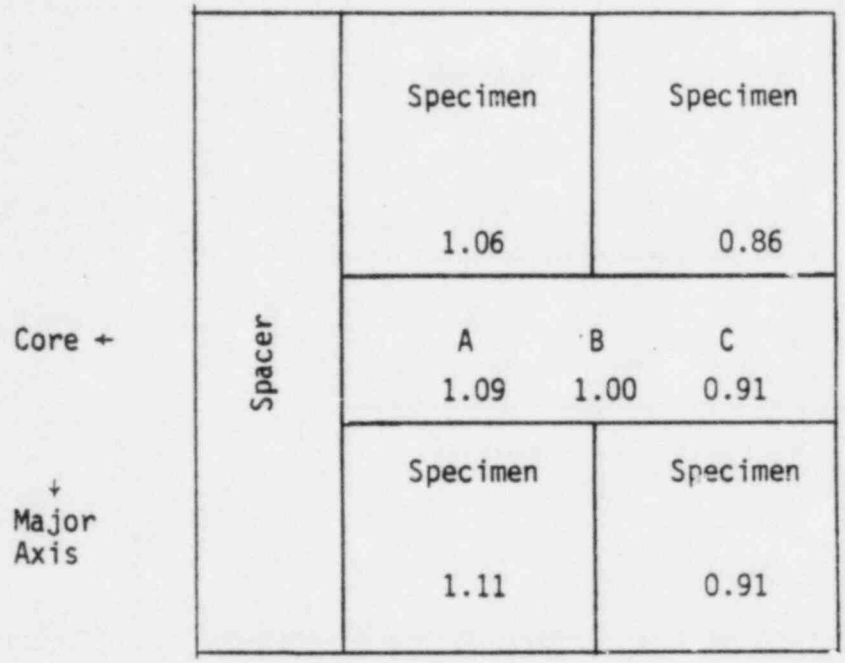

A, B, C = dosimeter wire positions

Figure 3-5. Axial Shape of Fast Flux at the Pressure Vessel Surface

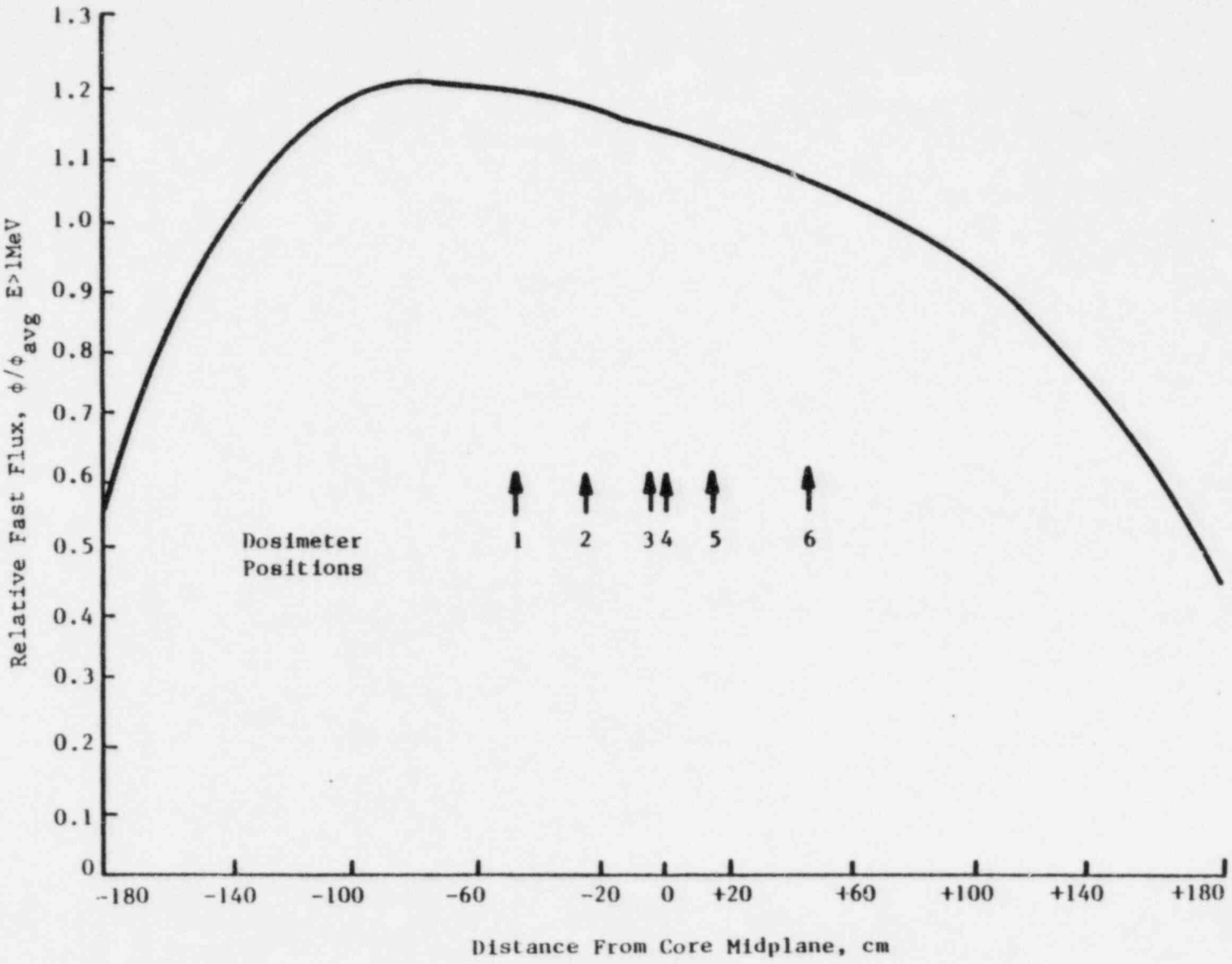

Figure 3-6. Radial Gradient of Fast Flux Through the Pressure Vessel

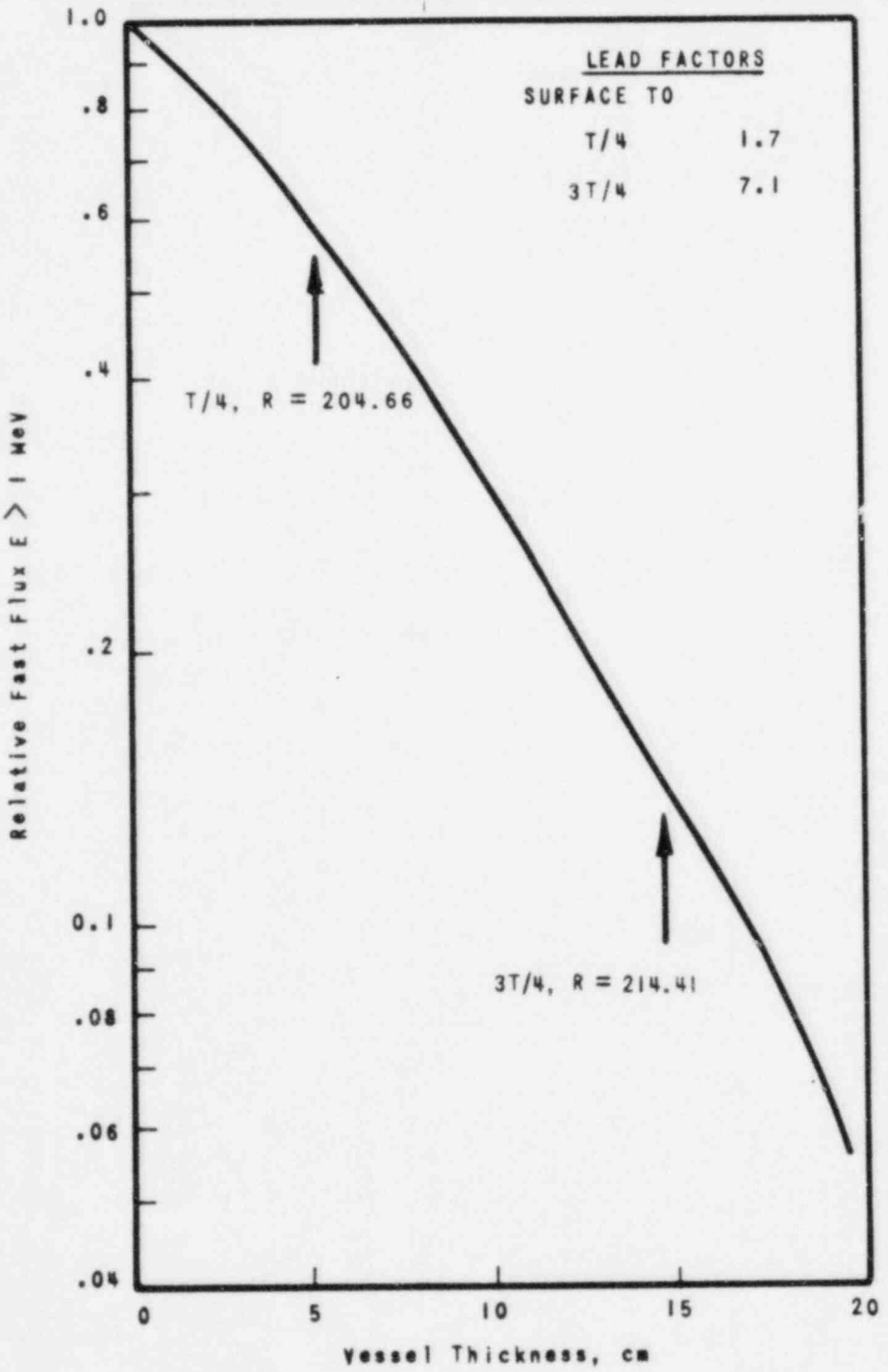

Figure 3-7. Azimuthal Gradient of Fast Flux at the Pressure Vessel Inside Surface

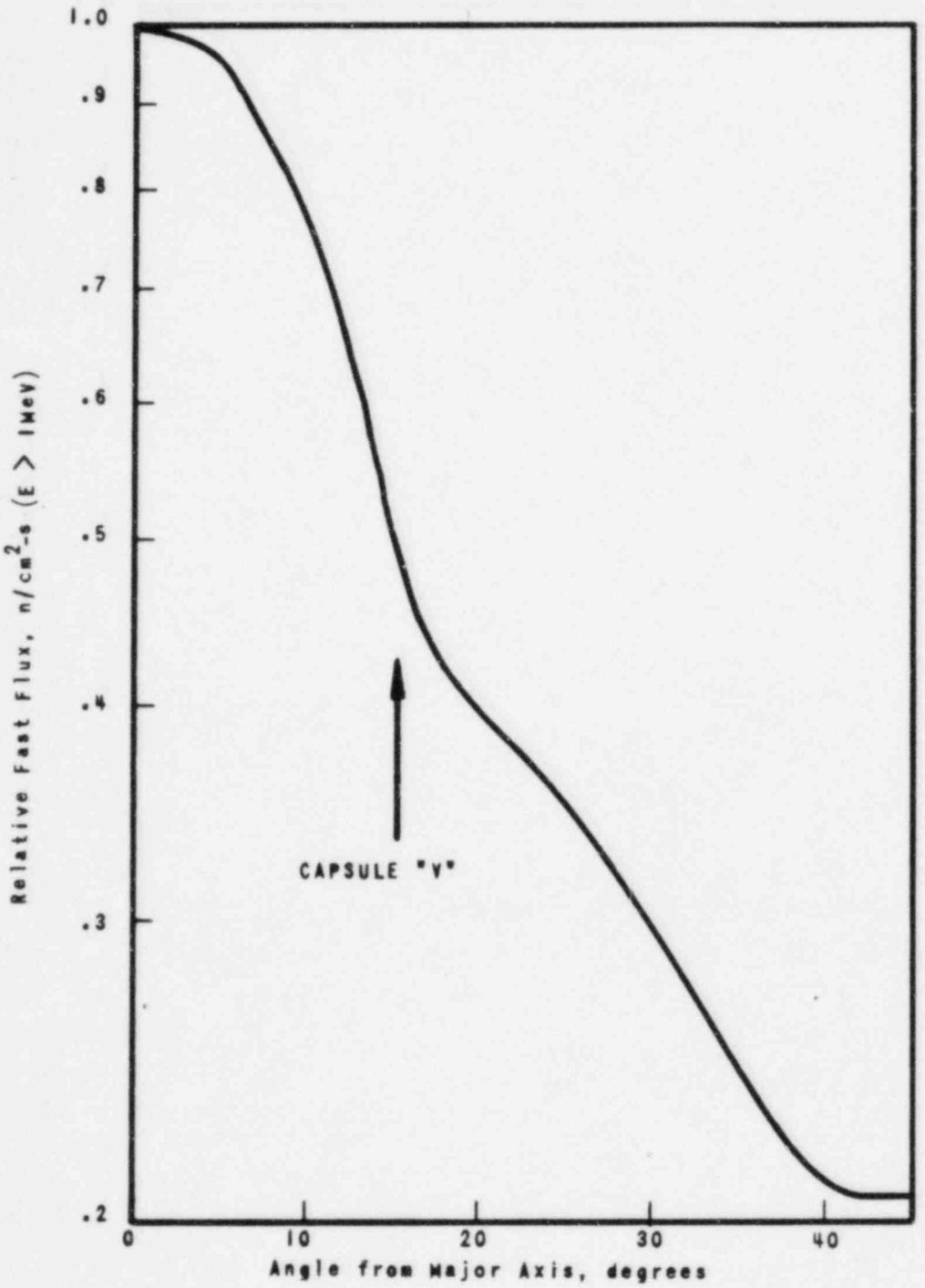

4. CAPSULE RESULTS

4.1. Tensile Properties

Table 4-1 compares irradiated and unirradiated tensile properties. At both room and elevated temperatures, the ultimate and yield strength changes in the base metal as a result of irradiation and the corresponding changes in ductility are within the range expected. There is some strengthening, as indicated by increases in ultimate and yield strength and small decreases in ductility properties. Some of the changes observed in the data are so small as to be considered within experimental error. The relative changes in the properties of the base metal at room temperature are similar to those observed for the weld metal, indicating similar sensitivity as the base metal to irradiation damage. These observations are further supported by the fact that the base metal chemistry contains similar quantities of those elements contained in the weld metal that are believed to influence radiation sensitivity. In both cases, the changes in tensile properties are not significant relative to the analysis of the reactor vessel materials at this period in service life. Moreover the Charpy data govern the adjustments to pressure-temperature heatup and cooldown curves.

4.2. Charpy Impact Properties

The behavior of the Charpy V-notch data is more significant to the calculation of the reactor system's operating limitations. Table 4-2 compares the observed changes in irradiated Charpy impact properties to the predicted changes.

The 50 ft-lb transition shift for the base metal showed a dependence on orientation. The material properties transverse to the working direction (axial) exhibited a greater sensitivity to radiation damage than the properties parallel to the working direction (tangential). In both cases, the change in properties was poorly predicted. The weld metal shift was also

significantly less than that predicted using Regulatory Guide 1.99. Similar differences were observed for the 30 ft-lb transition temperature shift except that the magnitude of the difference between the observed and predicted increased relative to the differences at the 50 ft-lb level.

The less-than-ideal comparison may be attributed to a number of factors. The spread in the data of the unirradiated material combined with a minimum of data points to establish the irradiated material curve. Under these conditions, the comparison indicates that the estimated curves in Regulatory Guide 1.99 for low-copper materials and at low fluence levels are overly conservative for predicting the tangential 50 ft-lb transition temperature shifts for all the materials.

The 30 ft-lb transition temperature shifts for the base metal is not in good agreement with the values predicted according to Regulatory Guide 1.99, although it would be expected that these values should exhibit better comparison when it is considered that a major portion of the data used to develop Regulatory Guide 1.99 was taken at the 30 ft-lb temperature.

The increase in the 35 mil lateral expansion transition temperature is compared to the shift in RT_{NDT} curve data in a manner similar to the comparison made for the 30 ft-lb transition temperature shift. These data show a behavior similar to that observed from the comparison of the observed and predicted 50 ft-lb and 30 ft-lb transition data.

The transition temperature measurements for the weld metal are not in agreement with the predicted shift. This can be attributed to the chemistry of the weld metal (low copper) as compared to the nominal chemistry of normal weld metal (medium to high copper) for which the prediction curves were developed. This being the case, it would not be expected that the current prediction techniques would apply to this class of weld metal.

The less than ideal comparison may be attributed in part to the combination of a spread in the data of the unirradiated material and the minimum number of data points available to establish the irradiated curve. These two variables can contribute to increasing the error between the observed and predicted values. Under these conditions, the comparison indicates that the estimating curves in Regulatory Guide 1.99 for low-copper materials at low

fluence levels are overly conservative for predicting the transition temperature shifts.

The data for the decrease in Charpy upper shelf energy (USE) with irradiation showed an interesting contrast when compared to the predicted values for the base metal. The decrease in upper shelf energy for the axial orientation was underpredicted while the tangential properties were greatly overpredicted. By comparison, the weld metal value, although underpredicted, is in the same relative range with the predicted values. Again, in view of the lack of data for low-copper weldments at low fluence values that were used to develop the estimating curves, the predictive techniques should improve as additional data are obtained from which better prediction curves can be developed.

Results from other capsules' evaluations indicate that the RT_{NDT} estimating curves have inaccuracies at the low neutron fluence levels ($<5 \times 10^{18}$ n/cm^2). This inaccuracy is attributed to the limited data at the low fluence values and to the fact that the majority of the data used to define the curves in Regulatory Guide 1.99 are based on the shift at 30 ft-lb. For the materials used in reactor vessels, the shifts measured at 50 ft-lb/35 mils lateral expansion (MLE) are expected to be higher than those measured at 30 ft-lb. The significance of the shifts at 50 ft-lb and/or 35 MLE is not well understood at present, especially for materials having USEs that approach the 50 ft-lb level and/or the 35 MLE level. Fortunately, these materials, all of which exhibit this characteristic, no longer have to be evaluated at transition energy levels of 50 ft-lb.

The lack of consistent agreement of the change in Charpy USE is further support of the inaccuracy of the prediction curves at the lower fluence levels. Although the prediction curves are not always conservative in that they do not predict a larger drop in USE than is observed for a given fluence and copper content, the lack of agreement is small and may be a function of material history. These data support the contention that the USE drop curves must be modified as more reliable data become available; until that time, the design curves used to predict the decrease in USE have adequate conservatism as currently used for regulations of the affected reactor pressure vessels.

Table 4-1. Comparison of Tensile Test Results

	Room temp test		Elevated temp test	
	Unirr	Irrad	550F	550F
Base Metal				
Fluence, 10^{18} n/cm^2 (>1 MeV)	0	2.41	0	2.41
Ult. tensile strength, ksi	102.0	104.5	97.2	98.7
0.2% yield strength, ksi	84.9	85.6	75.8	90.1
Uniform elongation, %	13.2	7.5	11.5	5.1
Total Elongation, %	19.0	18.4	18.1	13.3
RA, %	48.0	45.0	48.0	51.0
Weld Metal				
Fluence, 10^{18} n/cm^2 (>1 MeV)	0	2.41	0	2.41
Ult. tensile strength, ksi	86.0	91.6	80.1	--
0.2% yield strength, ksi	76.1	78.6	63.9	--
Uniform elongation, %	14.2	6.2	11.9	--
Total elongation, %	24.2	19.7	21.5	--
RA, %	69	64	62	--

Table 4-2. Observed Versus Predicted Changes in Irradiated Charpy Impact Properties

Material		
Increase in 30 ft-lb trans temp, F	Observed	Predicted[a]
Base material		
Axial	9	59
Tangential	9	59
Heat-affected zone	10	59
Weld metal	2	46
Increase in 50 ft-lb trans temp, F		
Base material		
Axial	28	59
Tangential	-4	59
Heat-affected zone	5	59
Weld metal	11	46
Increase in 35 MLE trans temp, F		
Base material		
Axial	18	59[b]
Tangential	-1	59[b]
Heat-affected zone	16	59[b]
Weld metal	-10	46[b]
Decrease in Charpy USE, ft-lb		
Base material		
Axial	13	10
Tangential	0	16
Heat-affected zone	6	13
Weld metal	23	19

[a]These values predicted per Regulatory Guide 1.99, Revision 1.

[b]Based on the assumption that MLE as well as 30 ft-lb transition temperature is used to control the shift in RT_{NDT}.

5. DETERMINATION OF PRESSURE-TEMPERATURE LIMITS

The pressure-temperature limits of the reactor vessel shell course region of North Anna Unit 2 are established in accordance with the requirements of 10 CFR 50, Appendix G. The methods and criteria employed to establish operating pressure and temperature limits are described in topical report BAW-10046.[4] The objective of these limits is to prevent nonductile failure during any normal operating condition, including anticipated operation occurrences and system hydrostatic tests. The loading conditions of interest include the following:

1. Normal operations, including heatup and cooldown.
2. Inservice leak and hydrostatic tests.
3. Reactor core operation.

The major components of the reactor vessel shell course region have been analyzed in accordance with 10 CFR 50, Appendix G. The reactor vessel outlet nozzle and the beltline region have been identified as the areas of the reactor vessel shell course region that regulate the pressure-temperature limits. The reactor vessel outlet nozzle affects the pressure-temperature limit curves of the first several service periods. This is due to the high local stresses at the inside corner of the nozzle, which can be two to three times the membrane stresses of the shell. After the first several years of neutron radiation exposure, the RT_{NDT} of the beltline region materials will be high enough that the beltline region of the reactor vessel will start to control the pressure-temperature limits. For the service period for which the limit curves are established, the maximum allowable pressure as a function of fluid temperature is obtained through a point-by-point comparison of the limits imposed by the outlet nozzle and the beltline region. The maximum allowable pressure is taken to be the lower of two calculated pressures.

The limit curves for North Anna Unit 2 are based on the predicted values of the adjusted reference temperatures of all the beltline region materials at the end of 10 EFPY. The 10th EFPY was selected because it is estimated that the second surveillance capsule will be withdrawn at the end of the refueling cycle when the estimated fluence corresponds to approximately 10 EFPY. The time difference between the withdrawal of the first and second surveillance capsule provides adequate time for reestablishing the operating pressure and temperature limits for the period of operation between the second and third surveillance capsule withdrawals.

The unirradiated impact properties were determined for the surveillance beltline region materials in accordance with 10 CFR 50, Appendixes G and H. For the other beltline region materials for which the measured properties are not available, the unirradiated impact properties and residual elements, as originally established for the beltline region materials, are listed in Table A-1. The adjusted reference temperatures are calculated by adding the predicted radiation-induced ΔRT_{NDT} and the unirradiated RT_{NDT}. The design curves of Regulatory Guide 1.99* were used to predict the radiation-induced ΔRT_{NDT} values as a function of the material's copper and phosphorus content and neutron fluence. Figure 5-1 illustrates the calculated peak neutron fluence at several locations through the reactor vessel beltline region wall as a function of exposure time. The neutron fluence values of Figure 5-1 are the predicted fluences, which have been demonstrated (section 3) to be conservative.

The neutron fluences and adjusted RT_{NDT} values of the beltline region materials at the end of the 10th EFPY are listed in Table 5-1. The neutron fluences and adjusted RT_{NDT} values are given for the 1/4T and 3/4T vessel wall locations. The assumed RT_{NDT} of the outlet nozzle steel forgings is that shown in Table A-1.

Figure 5-2 shows the reactor vessel's pressure-temperature limit curve for normal heatup. This figure also shows the core criticality limits as required by 10 CFR 50, Appendix G. Figures 5-3 and 5-4 show the vessel's pressure-temperature limit curve for normal cooldown and for heatup during

- - - - -

*Revision 1, January 1976.

inservice leak and hydrostatic tests, respectively. All pressure-temperature limit curves are applicable up to the 10th EFPY. Protection against nonductile failure is ensured by maintaining the coolant pressure below the upper limits of the pressure-temperature limit curves. The acceptable pressure and temperature combinations for reactor vessel operation are below and to the right of the limit curve. The reactor is not permitted to go critical until the pressure-temperature combinations are to the right of the criticality limit curve. To establish the pressure-temperature limits for protection against nonductile failure, the limits presented in Figures 5-2 through 5-4 must be adjusted by the pressure differential between the point of system pressure measurement and the pressure on the reactor vessel controlling the limit curves.

Table 5-1. Data for Preparation of Pressure-Temperature Limit Curves for North Anna Unit 2 -- Applicable Through 10 EFPY[a]

Material ident		Beltline region location	Weldment location			Unirr RT_{NDT}, F	Chemistry		Neutron fluence at end of 10 EFPY (E>1 Mev), n/cm^2		Radiation induced RT_{NDT} at end of 10 EFPY, F[b]		Adjusted RT_{NDT} at end of 10 EFPY, F	
Heat No.	Type		Core midplane to weld CL, cm	Location from major axis, degrees	Weld 1/4T location		Copper content %	Phosphorus content %	At 1/4T	At 3/4T	At 1/4T	At 3/4T	At 1/4T	At 3/4T
990698 / 291396	SA508,Cl.2	Upper shell	--	--	--	9	0.08	0.010	8.5E18	2.1E18	46	23	55	32
990496 / 292429	SA508,Cl.2	Intermediate shell	--	--	--	75	0.09	0.010	9.4E18	2.3E18	58	29	133	104
990633 / 207355	SA508,Cl.2	Lower shell	--	--	--	56	0.13	0.013	9.4E18	2.3E18	112	55	168	111
--	Weld metal	Mid. circum. (100%)	-50.8	--	yes	-48	0.088	0.017	9.4E18	2.3E18	90	45	42	-3

(a) All data for material identification, locations, initial properties, and chemical composition were obtained from the Final Safety Analysis Report.

(b) Adjustment in RT_{NDT} determined in accordance with Regulatory Guide 1.99, Rev 1, April 1977.

Figure 5-1. Predicted Fast Neutron Fluences at Various Locations Through Reactor Vessel Wall for 32 EFPY

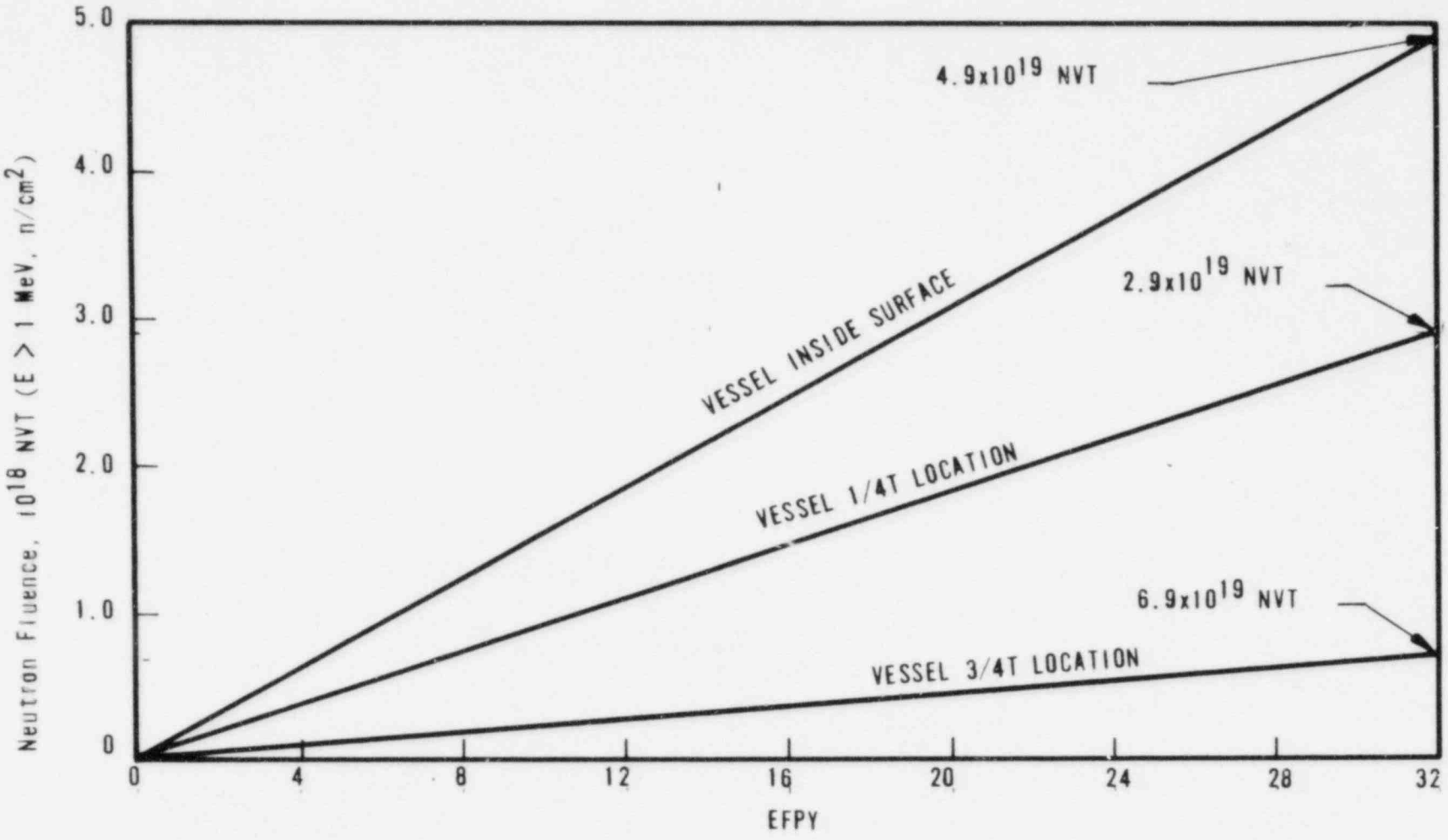

Figure 5-2. Reactor Vessel Pressure-Temperature Limit Curves for Normal Operation - Heatup, Applicable for First 10 EFPY

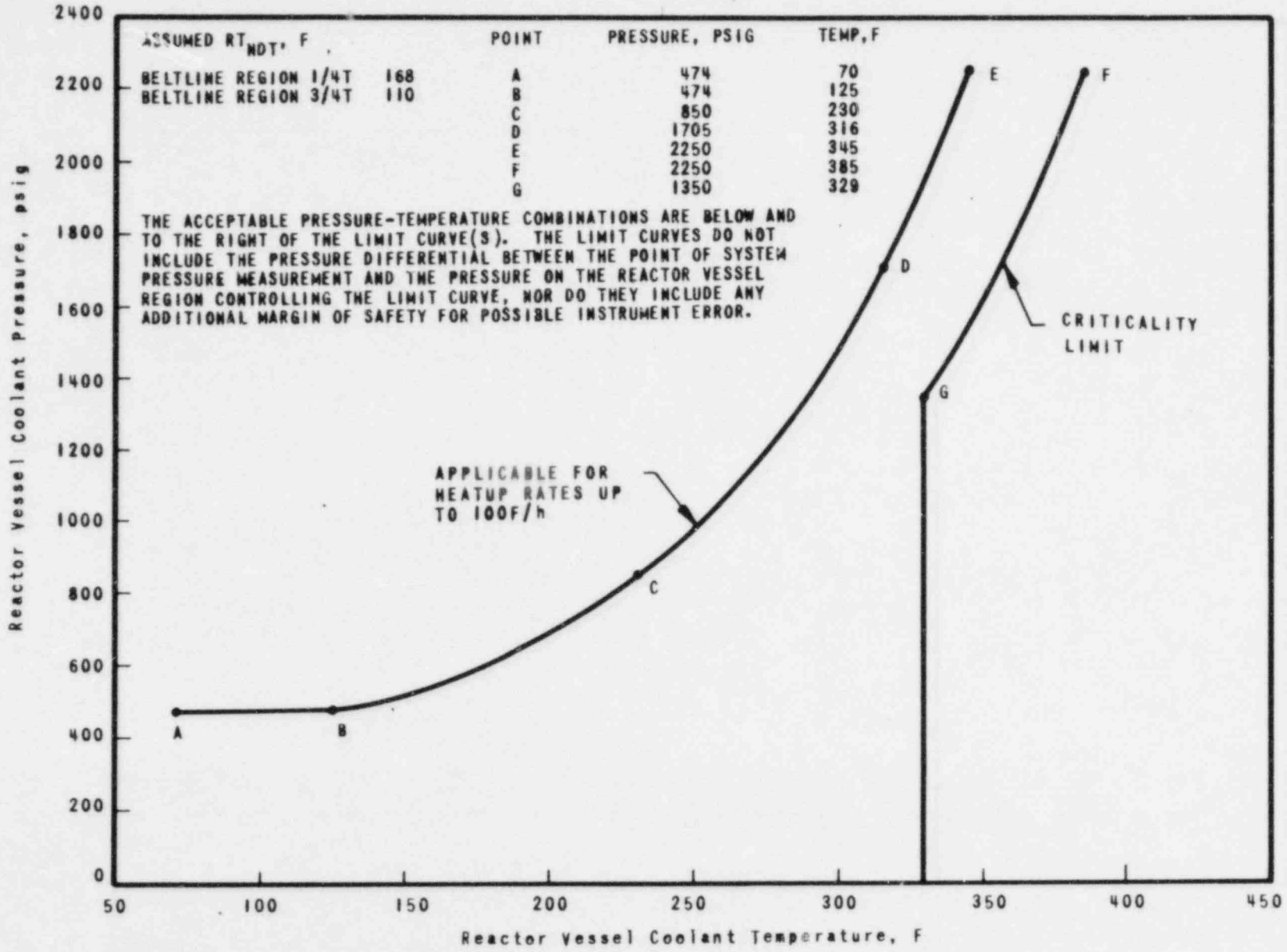

Figure 5-3. Reactor Vessel Pressure-Temperature Limit Curve for Normal Operation - Cooldown, Applicable for First 10 EFPY

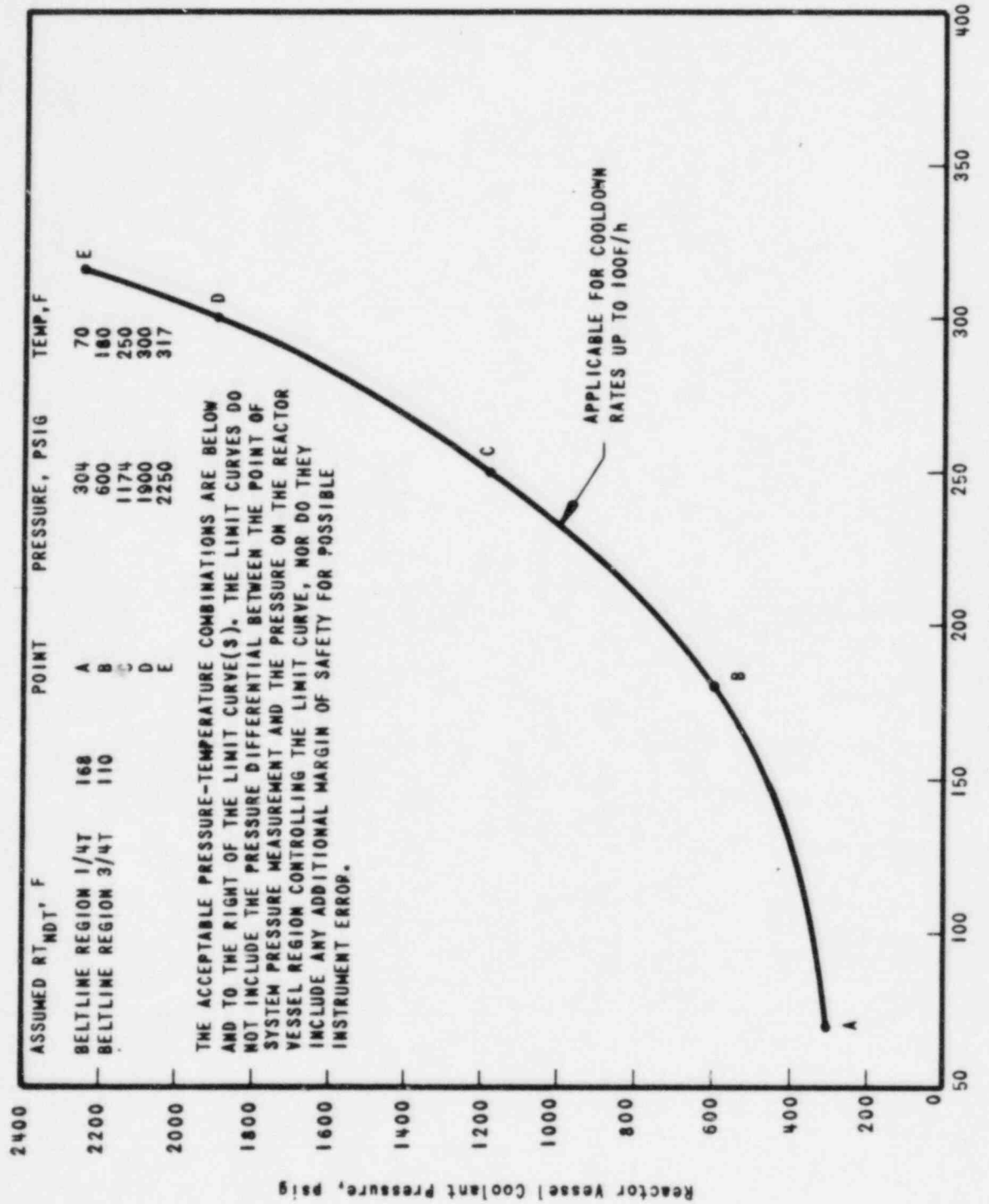

Figure 5-4. Reactor Vessel Pressure-Temperature Limit Curve for Inservice Leak and Hydrostatic Tests, Applicable for First 10 EFPY

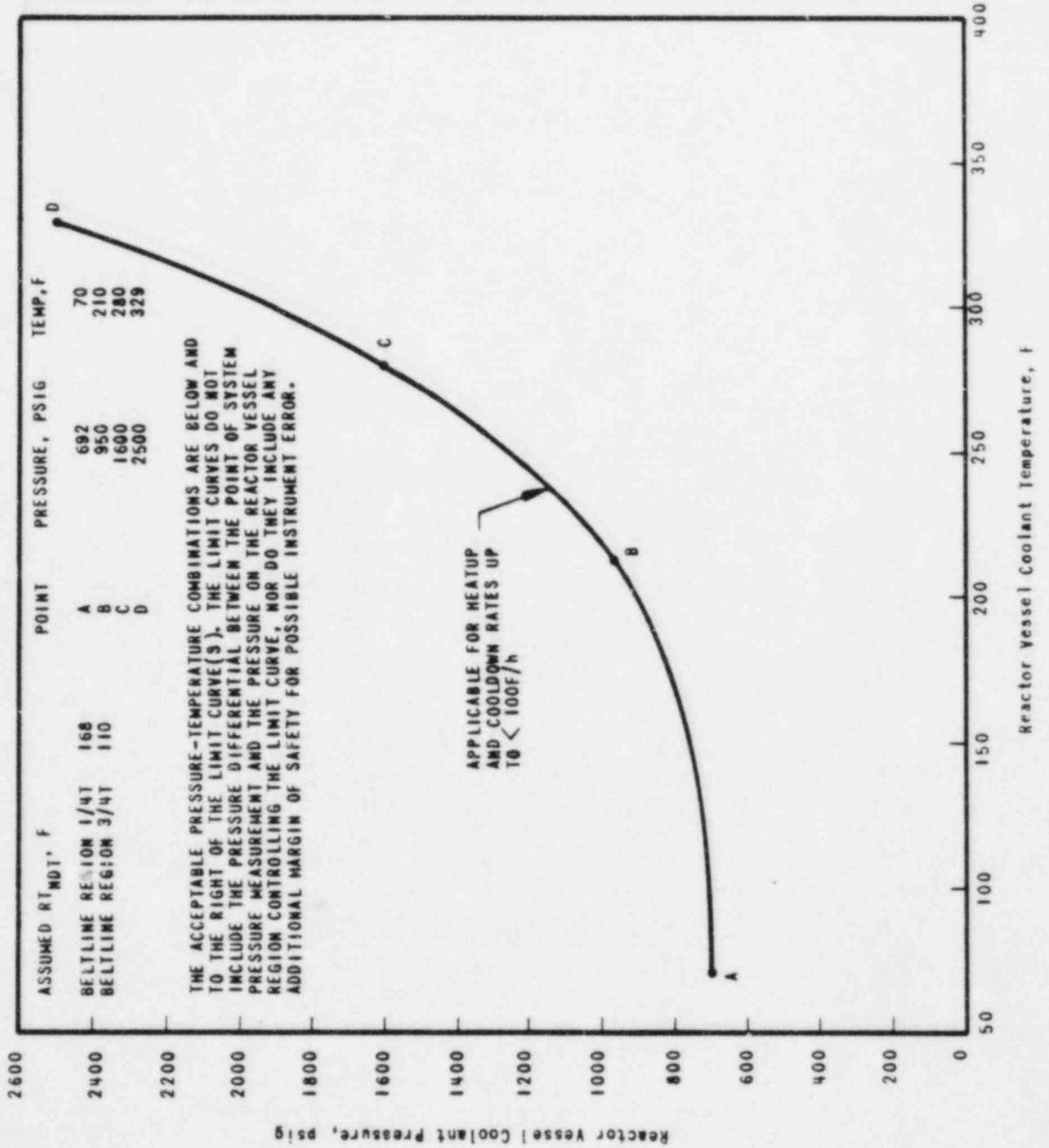

6. SUMMARY OF RESULTS

The analysis of the reactor vessel material contained in North Anna Unit 2, Capsule V, led to the following conclusions:

1. The capsule received an average fast fluence of 2.41 x 10^{18} n/cm^2 (E > 1 MeV). The predicted fast fluence for the reactor vessel inside wall location at the end of the first fuel cycle is 1.84 x 10^{18} n/cm^2 (E > 1 MeV).

2. The fast fluence of 2.41 x 10^{18} n/cm^2 (E > 1 MeV) increased the RT_{NDT} of the reactor vessel core region shell materials in the capsule to a maximum of 66F based on the shell forging axial orientation unirradiated data as shown in Figure C-1.

3. Based on the ratio of the fast flux at the surveillance capsule location to that at the vessel wall, the projected fast fluence that the North Anna Unit 1 reactor pressure vessel will receive in 32 EFPY operation is 4.9 x 10^{19} n/cm^2 (E > 1 MeV).

4. The increase in the transition temperature for the base plate material was conservative compared to that predicted by the currently used design curves of ΔRT_{NDT} versus fluence.

5. The increase in the transition temperature for the weld metal was not in good agreement with that predicted by the currently used design curves of ΔRT_{NDT} versus fluence.

6. The current techniques used for predicting the change in Charpy impact upper shelf properties due to irradiation are not consistent when compared with the changes observed for the various materials.

7. The analysis of the neutron dosimeters demonstrated that the analytical techniques used to predict the neutron flux and fluence were accurate.

8. The thermal monitors indicated that the capsule design was satisfactory for maintaining the specimens within the desired temperature range.

7. CERTIFICATION

The specimens were tested, and the data obtained from Virginia Electric & Power Company's North Anna Unit 2 surveillance Capsule V were evaluated using accepted techniques and established standard methods and procedures in accordance with the requirements of 10 CFR 50, Appendixes G and H.

A. L. Lowe, Jr., PE 8 Dec. 1983
A. L. Lowe, Jr., PE Date
Project Technical Manager

This report has been reviewed for technical content and accuracy.

John D. Aadland 12/8/83
J. D. Aadland Date
Materials & Chemical Engineering

APPENDIX A

Reactor Vessel Surveillance Program
Background Data and Information

1. Material Selection Data[1]

The data used to select the materials for the specimens in the surveillance program, in accordance with E185-73 are shown in Table A-1. The locations of these materials within the reactor vessel are shown in Figure A-1.

2. Surveillance Materials[1]

The Rotterdam Dockyard Company supplied the Westinghouse Electric Corporation with sections of SA508 Class 2 forging used in the core region of the North Anna Unit 1 reactor pressure vessel for the Reactor Vessel Material Surveillance Program. The sections of material were removed from a 10-inch lower shell course forging 04 of the pressure vessel heat treated as shown in Table A-1. The Rotterdam Dockyard Company also supplied a weldment made from sections of forging 04 and adjoining lower shell course forging 03 using weld wire representative of that used in the original fabrication. The forgings were produced by Rheinstahl Huttenwecke. The heat treatment history and quantitative chemical analysis of the pressure vessel surveillance material are presented in Tables A-1 and A-2, respectively.

3. Capsule Identification[1]

The capsules used in the North Anna Unit 2 surveillance program are identified and specimen tabulations are given in Tables A-3 and A-4.

Table A-1. Unirradiated Properties and Residual Element Content Data of Beltline Region Materials Used for Selection of Surveillance Program Materials - North Anna Unit 2*

Comp.	Heat No.	Material type	Chemistry Cu, %	Chemistry P, %	NDTT F	Minimum temperatures for 50 ft-lb, F: Parallel to major working direct.	Minimum temperatures for 50 ft-lb, F: Normal to major working direct.	RT_{NDT}, F	Average upper shelf, (ft-lb): Parallel to major working direct.(a)	Average upper shelf, (ft-lb): Normal to major working direct.
Upper shell	990598/291396	A508,Cl.2	0.08	0.010	+5	49	69(b)	9	86	
Inter-mediate shell	990496/292429	A508,Cl.2	0.09	0.010	-49	49	135(c)	75(c)	85	74(c)
Lower shell	990533/207355	A508,Cl.2	0.13	0.013	-13	31	116(c)	56(c)	92	80(c)
Weld		Weld	0.088	0.017	-67		12	-48		107
Heat-affected zone					-49		-20	-49		125

(a)Average energy at highest test temperatures ($\leq$68°F) -- % shear not reported.

(b)Estimated temperatures based on NRC Regulatory Standard Review Plan, Branch Technical Position MTEB 5-2.

(c)Average transverse data obtained from surveillance program.

*Data obtained from the Final Safety Analysis Report.

Table A-2. Heat Treatment History

Material	Temperature, F	Time, h	Coolant
Lower shell forging 04, Heat No. 990496/292424	1688-1697	2-1/2	Water-quenched
	1220-1229	6.0	Furnace-cooled to 842 F
	1130±25	14-3/4	Furnace cooled
Weld metal	1130 ± 25	13-1/2	Furnace-cooled

Table A-3. Quantitative Chemical Analysis, wt %

Element	Forging 04 heat No990496/292424 Westinghouse[a]	Rotterdam dock analysis	W weld metal analysis
C	0.19	0.19	0.08
S	0.011	0.015	0.011
N_2	0.011	-	0.011
Co	0.003	0.011	<0.002
Cu	0.11	0.09	0.088
Si	0.25	0.21	0.25
Mo	0.60	0.63	0.49
Ni	0.86	0.80	0.084
Mn	0.76	0.67	1.82
Cr	0.35	0.34	0.042
V	0.031	0.02	0.002
P	0.018	0.010	0.017
Sn	0.016	-	0.004
Al	0.023	0.017	0.015

[a]All elements not listed are less than 0.010 wt %.

Table A-4. Specimens in Surveillance Capsules Designated S,V,W, and Z

Material description	No. of test specimens/capsule		
	Tension	CVN impact	WOL
Forging 04			
Tangential		8	
Axial	2	12	4
Heat-Affected zone		12	
Weld metal	2	12	---
Total per capsule	4	44	4

Table A-5. Specimens in Surveillance Capsules Designated T,U,X, and Y

Material description	No. of test specimens/capsule		
	Tension	CVN impact	WOL
Forging 04			
Tangential		8	
Axial	2	12	
Heat-Affected zone		12	
Weld metal	2	12	4
Total per capsule	4	44	4

Figure A-1. Location and Identification of Materials Used in the Fabrication of the Core Belt Region of North Anna Unit 2 Reactor Pressure Vessel*

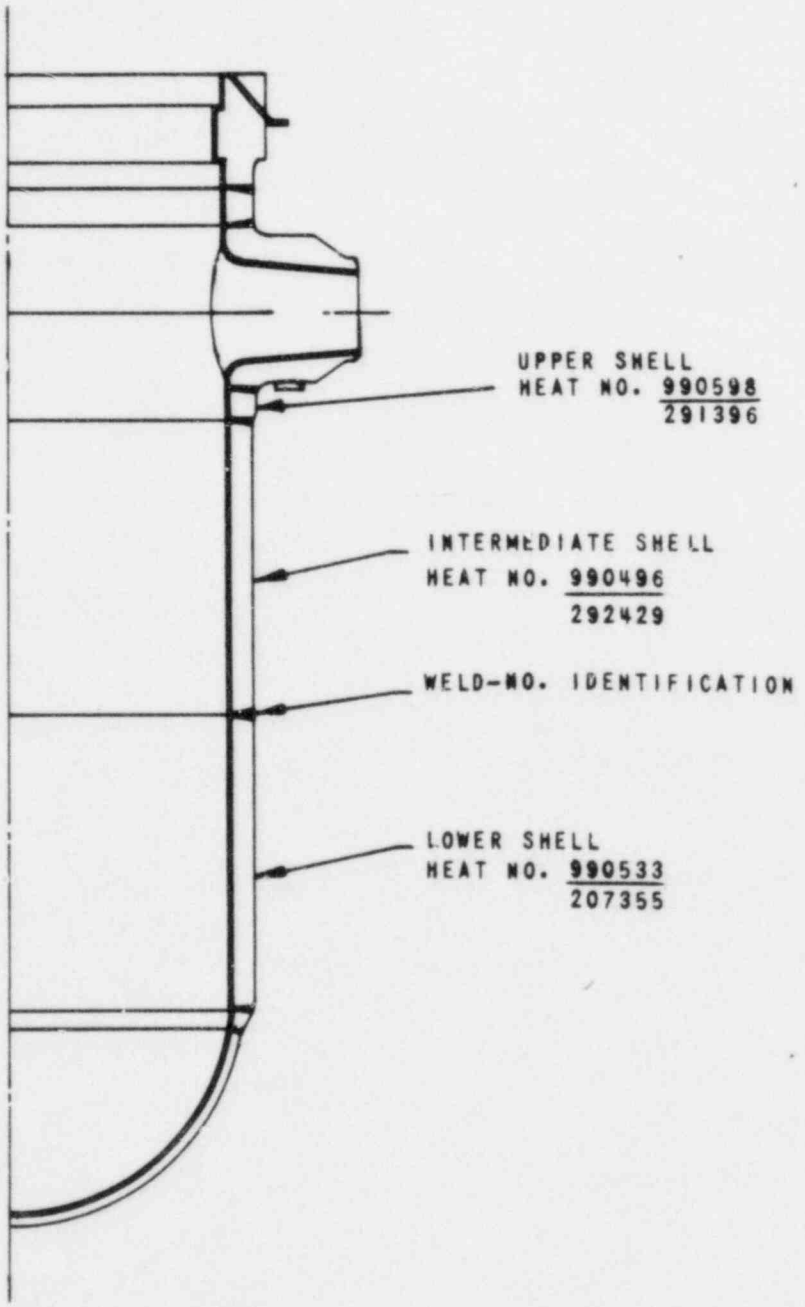

*Material identification and location obtained from the Final Safety Analysis Report.

APPENDIX B
Preirradiation Tensile Data[1]

Table B-1. Preirradiated Tensile Properties of Forging Material (Base Metal) and Weld Metal

Test temp, F	Strength, psi		Elongation, %		
	Yield	Ultimate	Uniform	Total	RA, %
Base Metal					
RT	84,800	101,600	13.1	20.2	56
RT	85,000	102,500	13.3	17.8	40
Average	84,900	102,000	13.2	19.0	48
300	77,700	95,500	10.9	16.8	46
300	77,600	94,800	10.1	16.6	53
Average	77,650	95,150	10.5	16.7	50
550	75,600	97,100	11.4	18.6	53
550	75,900	97,200	11.6	17.7	44
Average	75,750	97,150	11.5	18.1	48
Weld Metal					
RT	77,800	86,200	14.2	24.5	70
RT	74,400	85,700	14.2	23.9	68
Average	76,100	85,950	14.2	24.2	69
300	67,500	76,600	10.8	19.6	64
300	69,500	77,600	10.6	22.2	69
Average	68,500	77,100	10.7	20.9	66
550	64,000	80,100	12.7	22.7	67
550	63,700	80,000	11.1	20.3	58
Average	63,850	80,050	11.9	21.5	62

APPENDIX C

Preirradiation Charpy Impact Data[1]

Table C-1. Preirradiation Charpy V-Notch Impact Data for North Anna Unit 2 Reactor Pressure Vessel Surveillance Base Metal, Heat No. 990496/292424, Axial Orientation

Specimen No.	Test temp, F	Absorbed energy, ft-lb	Lateral expansion, mils	Shear fracture, %
WL1	-50.	14.0	6.0	<5.
WL2	-50.	4.0	0.0	<5.
WL3	-50.	4.0	0.0	<5.
WL4	15.	15.0	7.0	5.
WL5	15.	14.5	4.0	5.
WL6	15.	22.0	14.0	10.
WL7	75.	53.0	38.0	55.
WL8	75.	36.5	31.0	40.
WL9	75.	31.0	23.0	40.
WL10	120.	53.0	49.0	65.
WL11	120.	44.5	46.0	55.
WL12	120.	50.5	43.0	55.
WL13	210.	80.0	64.0	100.
WL14	210.	72.0	63.0	100.
WL15	210.	71.0	63.0	100.
WL16	300.	64.5	49.0	100.
WL17	300.	67.0	64.0	100.
WL18	300.	76.0	63.0	100.

Table C-2. Preirradiation Charpy V-Notch Impact Data for North Anna Unit 2 Reactor Pressure Vessel Surveillance Base Metal, Heat No. 990496/292424, Tangential Orientation

Specimen No.	Test temp, F	Absorbed energy, ft-lb	Lateral expansion, mils	Shear fracture, %
WT1	-50.	33.0	24.0	14.
WT2	-50.	16.0	9.0	10.
WT3	-50.	30.0	22.0	14.
WT4	15.	35.0	23.0	15.
WT5	15.	36.0	25.0	15.
WT6	15.	61.5	45.0	28.
WT7	50.	68.0	49.0	35.
WT8	50.	90.0	66.0	55.
WT9	50.	62.0	45.0	30.
WT10	100.	37.0	35.0	45.
WT11	100.	109.0	78.0	100.
WT12	100.	102.0	72.0	88.
WT13	150.	102.0	75.0	100.
WT14	150.	126.0	83.0	100.
WT15	150.	125.0	84.0	100.
WT16	212.	113.0	81.0	100.
WT17	212.	102.0	75.0	100.
WT18	212.	129.0	80.0	100.

Table C-3. Preirradiation Charpy V-Notch Impact Data for North Anna Unit 2 Reactor Pressure Vessel Surveillance Heat-Affected Zone Metal

Specimen No.	Test temp, F	Absorbed energy, ft-lb	Lateral expansion, mils	Shear fracture, %
WH1	-115.	5.0	1.0	8.
WH2	-115.	8.0	3.0	9.
WH3	-115.	15.0	9.0	15.
WH4	-35.	51.0	34.0	57.
WH5	-35.	50.0	32.0	52.
WH6	-35.	52.0	32.0	52.
WH7	32.	27.0	26.0	30.
WH8	32.	62.0	47.0	72.
WH9	32.	90.0	59.0	81.
WH10	68.	95.0	63.0	100.
WH11	68.	94.0	67.0	100.
WH12	68.	104.0	69.0	100.
WH13	140.	76.0	59.0	100.
WH14	140.	92.0	62.0	100.
WH15	140.	113.0	70.0	100.
WH16	212.	106.0	66.0	100.
WH17	212.	122.0	71.0	100.
WH18	212.	77.0	58.0	100.

Table C-4. Preirradiation Charpy V-Notch Impact Data for North Anna Unit 2 Reactor Pressure Vessel Core Region Weld Metal

Specimen No.	Test temp, F	Absorbed energy, ft-lb	Lateral expansion, mils	Shear fracture, %
WW1	-115.	11.0	7.0	13.
WW3	-115.	7.0	3.0	12.
WW2	-115.	6.0	1.0	9.
WW4	-55.	19.5	16.0	23.
WW5	-55.	18.5	12.0	20.
WW6	-55.	18.0	14.0	23.
WW7	-15.	43.5	39.0	41.
WW8	-15.	30.5	27.0	40.
WW9	-15.	43.0	35.0	42.
WW10	15.	76.5	59.0	72.
WW11	15.	69.0	55.0	70.
WW12	15.	77.0	63.0	73.
WW13	68.	83.0	64.0	77.
WW14	68.	91.0	73.0	85.
WW15	68.	88.0	74.0	85.
WW16	140.	109.0	87.0	100.
WW17	140.	116.0	89.0	100.
WW18	140.	108.0	82.0	100.

Figure C-1. Charpy Impact Data From Unirradiated Base Metal, Axial Orientation

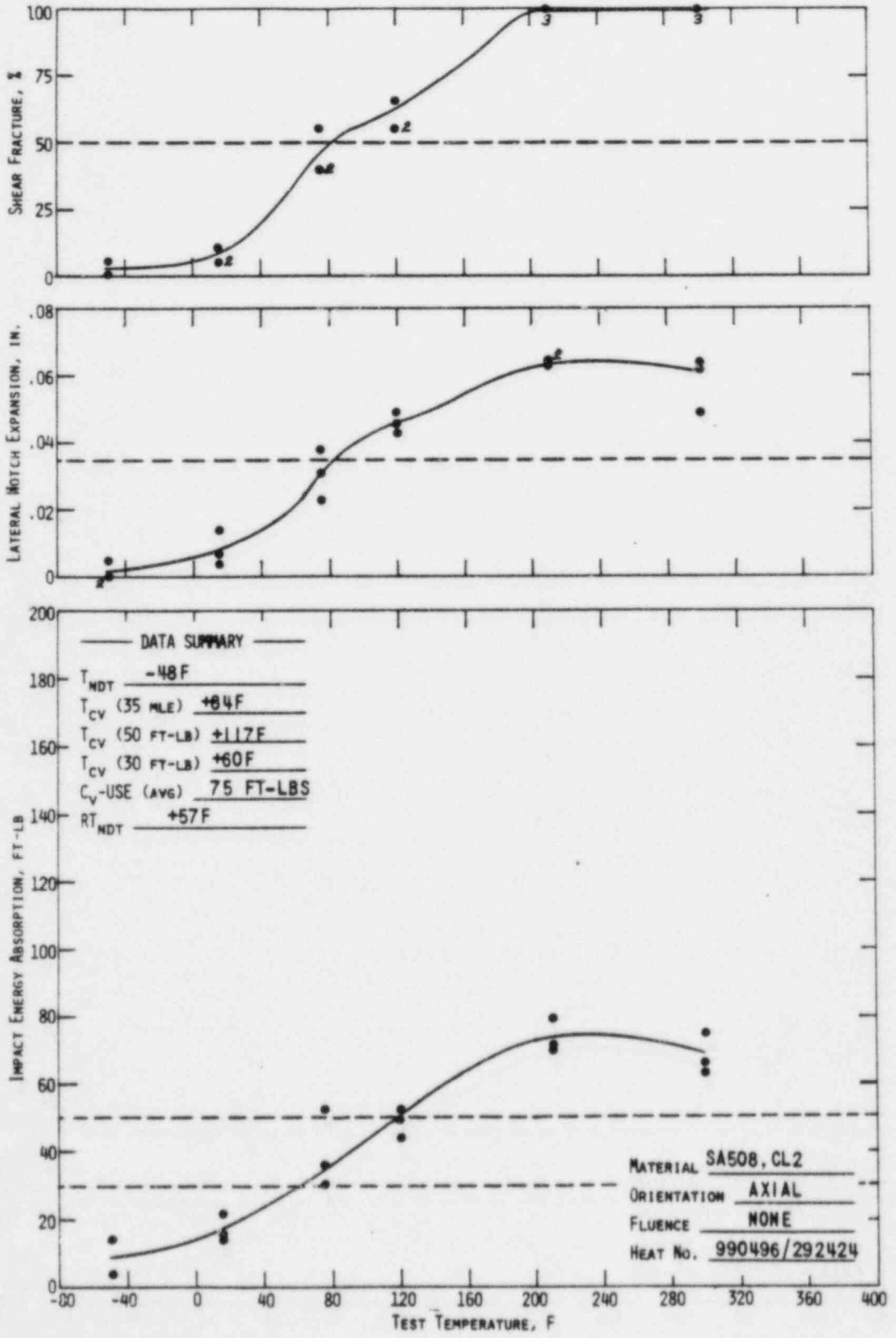

Figure C-2. Charpy Impact Data From Unirradiated Base Metal, Tangential Orientation

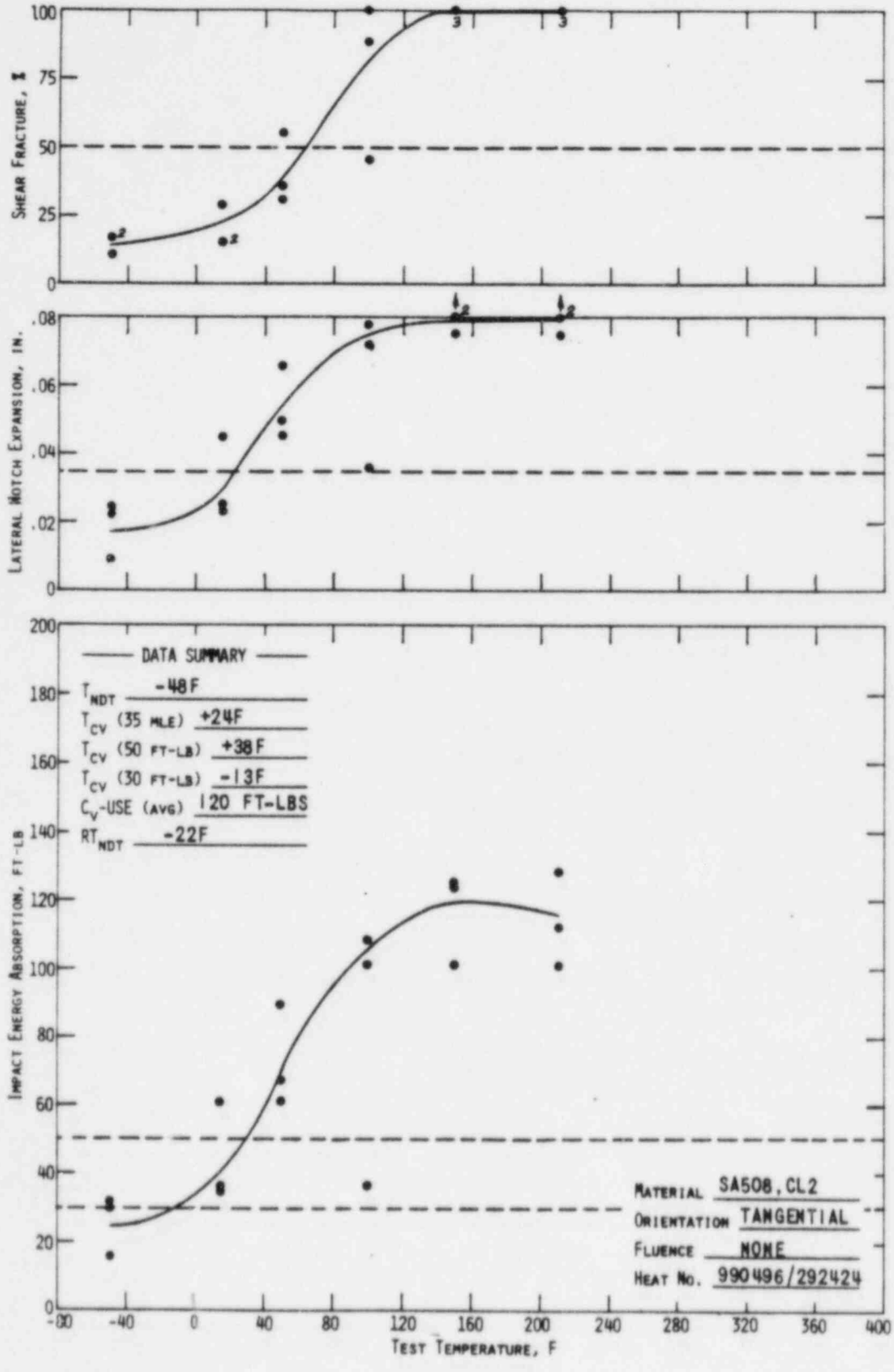

Figure C-3. Charpy Impact Data From Unirradiated Base Metal, Heat Affected Zone

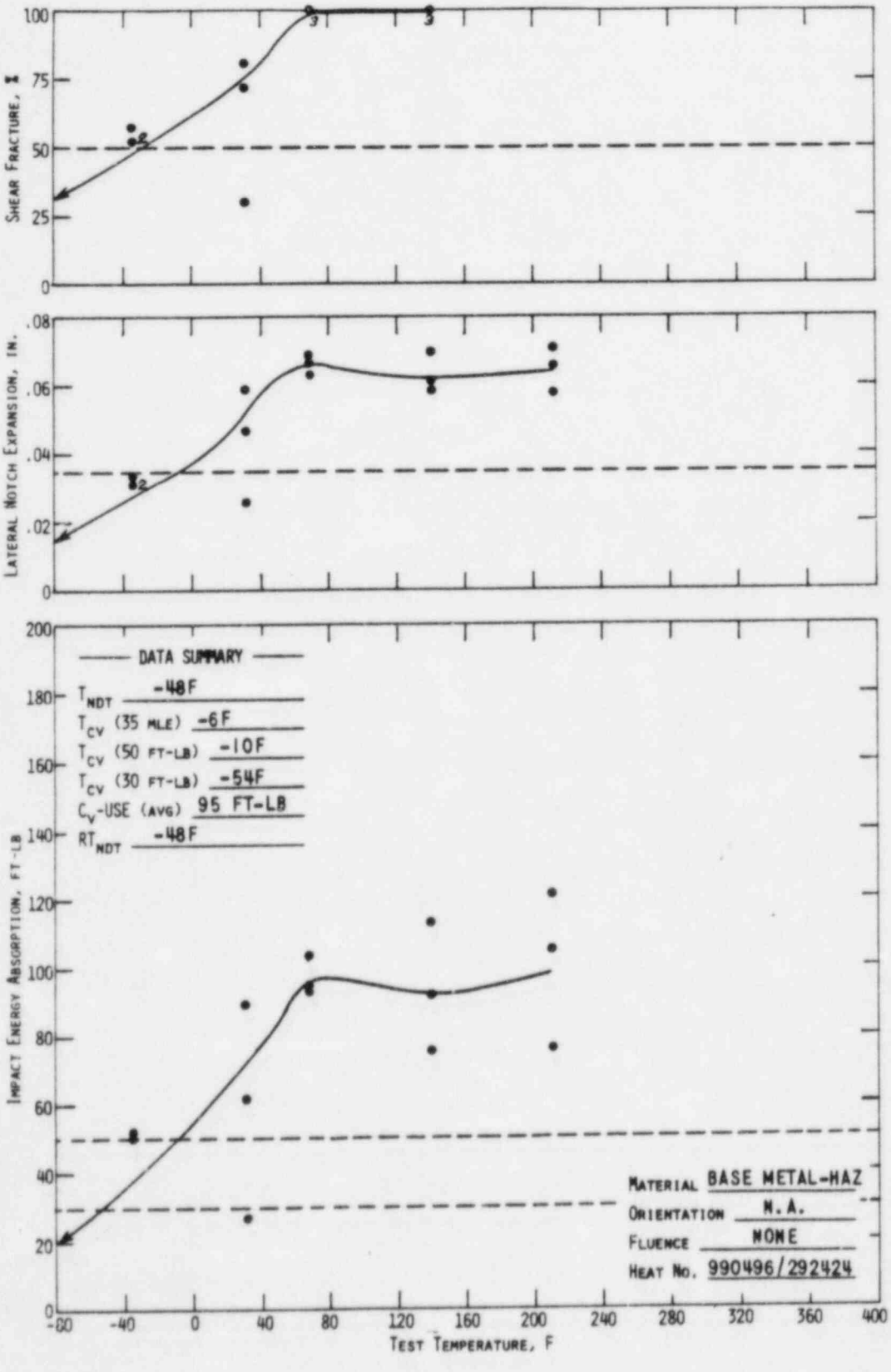

Figure C-4. Charpy Impact Data From Unirradiated Weld Metal

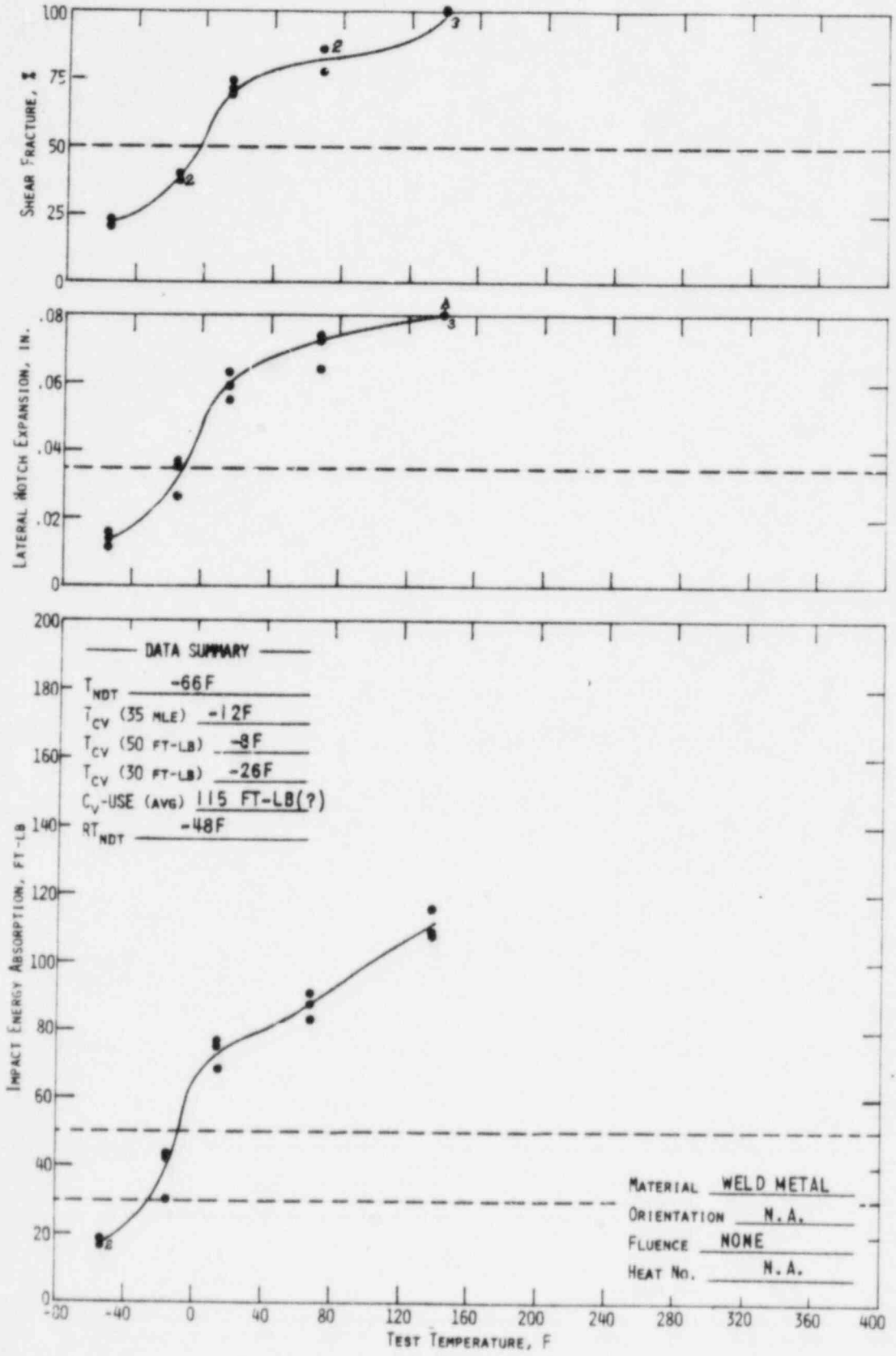

APPENDIX D
Threshold Detector Information

Table D-1. Dosimeter Specific Activities

Plant: North Anna Unit 2

Dosimeter: Cobalt-Aluminum

Dosimeter Location	Post irrad. wt, g	Reaction	Radio-nuclide	Nuclide activity, μCi	Specific Act.,[a] μCi/g	Activity[b,c] μCi/g of target
Bare:						
Top-Co	0.00884	$^{59}Co(n,\gamma)$	^{60}Co	1.986	224.7	149800
Bottom-Co	0.00828	$^{59}Co(n,\gamma)$	^{60}Co	1.921	232.0	154700
Cd Shielded:						
Top-Co	0.00870	$^{59}Co(n,\gamma)$	^{60}Co	0.6770	77.82	51880
Bottom-Co	0.00740	$^{59}Co(n,\gamma)$	^{60}Co	0.6826	92.24	61490

Table D-1. (Cont'd)

Plant: North Anna Unit 2

Dosimeter: Iron

Dosimeter Location	Post irrad. wt, g	Reaction	Radio-nuclide	Nuclide activity, μCi	Specific act.,[a] μCi/g	Activity[b,c] μCi/g of target
Top	0.05553	$^{54}Fe(n,p)$	^{54}Mn	2.710	48.80	838.5
		$^{58}Fe(n,\gamma)$	^{59}Fe	6.829	123.0	37270
Mid-Top	0.05531	$^{54}Fe(n,p)$	^{54}Mn	2.590	46.83	804.6
		$^{58}Fe(n,\gamma)$	^{59}Fe	6.790	122.8	37210
Mid	0.05238	$^{54}Fe(n,p)$	^{54}Mn	2.571	49.08	843.3
		$^{58}Fe(n,\gamma)$	^{59}Fe	6.132	117.1	35480
Mid-Bottom	0.05601	$^{54}Fe(n,p)$	^{54}Mn	2.691	48.04	825.4
		$^{58}Fe(n,\gamma)$	^{59}Fe	6.868	122.6	37150
Bottom	0.05215	$^{54}Fe(n,p)$	^{54}Mn	2.612	50.09	860.7
		$^{58}Fe(n,\gamma)$	^{59}Fe	6.272	120.3	36450

Table D-1. (Cont'd)

Plant: North Anna Unit 2

Dosimeter: Copper and Nickel

Dosimeter location	Post irrad. wt, g	Reaction	Radio-nuclide	Nuclide activity, μCi	Specific act.,(a) μCi/g	Activity(b,c) μCi/g of target
Copper:						
Mid-Top	0.06459	$^{63}Cu(n,\alpha)$	^{60}Co	0.08504	1.317	1.825
Mid	0.06637	$^{63}Cu(n,\alpha)$	^{60}Co	0.09286	1.399	2.045
Mid-bottom	0.05936	$^{63}Cu(n,\alpha)$	^{60}Co	0.07879	1.327	1.940
Nickel:						
Mid-Top	0.06532	$^{58}Ni(n,p)$	^{58}Co	69.22	1060	1564
		$^{60}Ni(n,p)$	^{60}Co	0.1247	1.909	7.297
Mid	0.05526	$^{58}Ni(n,p)$	^{58}Co	60.36	1092	1611
		$^{60}Ni(n,p)$	^{60}Co	0.1095	1.982	7.576
Mid-bottom	0.05658	$^{58}Ni(n,p)$	^{58}Co	60.30	1066	1573
		$^{60}Ni(n,p)$	^{60}Co	0.1086	1.919	7.336

Table D-1. (Cont'd)

Plant: North Anna Unit 2

Dosimeter: Uranium and Neptunium

Dosimeter Location	Post irrad. wt, g	Reaction	Radio-nuclide	Nuclide activity, μCi	Specific act.,(a) μCi/g	Activity(b,c) μCi/g of target
$^{238}U_3O_8$	0.00533	$^{238}U(n,F)$	^{95}Zr	0.3531	66.2	78.2
			^{103}Ru	0.4207	78.9	93.2
			^{106}Ru	0.09546	17.9	21.1
			^{137}Cs	0.01289	2.42	2.86
			^{144}Ce	0.2149	40.3	47.6
$^{237}NpO_2$	0.00718	$^{237}Np(n,F)$	^{95}Zr	3.846	536	609
			^{103}Ru	3.870	539	612
			^{106}Ru	0.7762	108	123
			^{137}Cs	0.1296	18.1	20.6
			^{144}Ce	1.840	256	291

Table D-1. (Cont'd)

Dosimeter Material Data

(a) These data are the disintegration rates per gram of wire as of 1200 hrs, 7 March 1982.

(b) These data are the disintegration rates per gram of target nuclide: viz., ^{238}U, ^{237}Np, ^{58}Ni, ^{60}Ni, ^{59}Co, ^{54}Fe, and ^{58}Fe.

(c) The following abundances and weight percents were used to calculate the disintegration rate per gram of target element:

^{238}U - 84.8 wt %; 99.9% target nuclide

^{237}Np - 88.1 wt %; 99.9% target nuclide

Ni - 100 wt %; 67.77% ^{58}Ni target nuclide
26.16 ^{60}Ni target nuclide

Co - 0.15 wt %; 100% ^{59}Co target nuclide

Fe - 100 wt %; 5.82% ^{54}Fe target nuclide
0.33% ^{58}Fe target nuclide

Cu - 100 wt %; 68.4% ^{63}Cu target nuclide

Table D-2. Dosimeter Activation Cross Sections[a]

G	Energy range, MeV		^{237}Np	^{238}U	^{58}Ni	^{53}Fe	^{63}Cu
1	13.3	-15.0	2.323	1.050	0.4830	0.4133	4.478 (-2)
2	10.0	-12.2	2.341	0.9851	0.5735	0.4728	5.361 (-2)
3	8.18	-10.0	2.309	0.9935	0.5981	0.4772	3.378 (-2)
4	6.36	-8.18	2.093	0.9110	0.5921	0.4714	1.246 (-2)
5	4.96	-6.36	1.541	0.5777	0.5223	0.4321	3.459 (-3)
6	4.06	-4.96	1.532	0.5454	0.4146	0.3275	6.348 (-4)
7	3.01	-4.06	1.614	0.5340	0.2701	0.2193	7.078 (-5)
8	2.46	-3.01	1.689	0.5272	0.1445	0.1080	3.702 (-6)
9	2.35	-2.46	1.695	0.5298	9.154 (-2)	5.613 (-2)	6.291 (-7)
10	1.83	-2.35	1.677	0.5313	4.856 (-2)	2.940 (-2)	1.451 (-7)
11	1.11	-1.83	1.596	0.2608	1.180 (-2)	2.948 (-3)	1.317 (-9)
12	0.55	-1.11	1.241	9.845 (-3)	6.770 (-4)	6.999 (-5)	0
13	0.111	-0.55	0.2341	2.432 (-4)	1.174 (-6)	1.578 (-8)	0
14	0.0033	-0.111	0.0069	3.616 (-5)	1.023 (-7)	1.389 (-9)	0

(a)ENDF/BV values flux-weighted with a fission spectrum combined with a 1/E intermediate energy distribution.

APPENDIX E

LRC-TP-78 (1-26-82)
Tension Testing of Solid Round Specimens

1. Introduction

This Technical Procedure describes the requirements for tension testing of solid, circular cross-section, metal specimens at room and elevated temperatures. Unless otherwise indicated, the room temperature tests conform to ASTM E8-81, "Standard Methods of Tension Testing of Metallic Materials," and the elevated temperature tests conform to ASTM E21-79, "Standard Recommended Practice for Elevated Temperature Tension Tests of Metallic Materials."

2. Operator Qualification

Tension test operators shall be qualified by training and experience and shall have demonstrated competence to perform the tests in accordance with this procedure to the satisfaction of the LRC Project Leader.

3. Test Specimen

Test specimens shall be solid, of circular cross-section, and generally conform to the shapes described in ASTM E8-81, Figures 8 and 9. For elevated temperature testing, specimens shall conform to the additional requirements of ASTM E21-79, Paragraph 7.6. Specimen length and diameter may be varied in accordance with project needs, however, the ratio of gage length to diameter shall be 4:1. Specimen ends beyond the gage length shall be of a shape and size compatible with the intended gripping device. The gage length shall be bounded by fiducial marks such that the fiducial marks may be measured after test to determine extension of the gage length. The method of placing fiducial marks shall be determined by the LRC Project Leader.

4. Equipment

4.1 Tension Testing Machine

4.1.1 The tension testing machine shall be in conformance with the requirements of ASTM E8-81, Paragraph 5.1.

4.1.2 The machine shall have sufficient capacity to load specimens to failure.

4.1.3 Gripping devices shall generally conform to ASTM E8-81, Figure 2 or 3, except that clevis-type grips to accommodate square-end pin-loaded specimens are permitted.

4.2 Extensometry

Extensometers shall be of class B-2 or better (ASTM E83-67).

4.3 Heating Apparatus

4.3.1 For elevated temperature testing, a furnace or oven shall be provided to heat specimens uniformly such that test temperature will be maintained to within ± 5F along the gage length of the specimen.

4.3.2 Temperature measurement shall be by thermocouples suitable for the temperature of the test. Thermocouple output shall be measured by potentiometers. The complete temperature measurement system shall be of sufficient accuracy and sensitivity to monitor the test temperature within the specified limits.

5. Calibration

5.1 Load

The load cell and its associated electronics shall be calibrated against standards traceable to the National Bureau of Standards (NBS) at least annually by a manufacturer's representative or similarly qualifed person.

5.2 Stroke

The stroke (displacement) monitoring portion of the tension test machine shall be calibrated at least annually against standards traceable to the NBS by a manufacturer's representative or similarly qualified person.

5.3 Strain

Extensometers, signal conditioners, and output recorders shall be calibrated at least annually against NBS traceable standards.

5.4 Temperature

5.4.1 Thermocouples or thermocouple wire shall be purchased with calibration traceable to NBS standards. Thermocouples shall be replaced at least after one year of service.

5.4.2 Potentiometers shall be calibrated at least annually against standards traceable to the NBS.

5.5 Dimensional Measurement

5.5.1 Micrometers used for diametral measurement shall be calibrated at least annually in accordance with LRC-TP-44 (2/7/78).

5.5.2 Calipers used for measurement of gage length changes in displacement shall be calibrated at least annually against NBS traceable standards.

5.5.3 Remotely operable measurement devices, such as video-micrometers, shall be calibrated at least annually against NBS traceable standards.

6. Tension Test Procedure

6.1 Specimen Measurement

The minimum cross-sectional area of the reduced section of the specimen shall be determined. The diameter at the ends of the reduced section shall not be less than the diameter at the center of the reduced section. Diameters shall be determined with a micrometer or comparable instrumentation.

6.2 Evaluated Temperature Test Set-up

For elevated temperature testing, the test set-up shall be in accordance with ASTM E21-79, paragraphs 9.3, 9.4, and 9.5.

6.3 Strain Rate

Except if designated otherwise by the LRC Project Leader, the strain rate shall be maintained at 0.005 ± 0.002/min to the 0.2% offset yield strength. The strain rate shall then be increased to 0.05 ± 0.01/min.

6.4 Temperature

Test temperature shall be as designated by the LRC Project Leader. Specimens shall be held at test temperature for at least 20 minutes before testing to assure achievement of thermal equilibrium.

7. Calculations

7.1 Yield Strength

7.1.1 Yield strength shall be determined by the 0.2% offset method.

7.1.2 The 0.2% offset is defined as a displacement equal to 0.002 times the specimen gage length.

7.1.3 Yield strength shall be determined from the load-displacement chart by drawing a straight line parallel to the elastic portion of the load-displacement curve extending from 0.2% offset on the zero load axis. The load at the intersection of this straight line with the load-displacement curve shall be taken as the "load at yield." This value shall then be divided by the original cross-sectional area to obtain the yield strength.

7.2 Tensile Strength

Tensile strength shall be determined by dividing the maximum load carried by the specimen during the tension test by the original cross-sectional area of the specimen.

7.3 Total Elongation

7.3.1 The change in length of the "gage length" due to testing shall be determined by fitting together the broken ends of the specimen and measuring the distance between the gage marks to, at least, the nearest 0.01 inch and subtracting the gage length from this value.

7.3.2 Total elongation shall be expressed as the percentage increase in gage length and obtained by dividing the change in length of the "gage length" by the gage length and multiplying by 100.

7.4 Uniform Elongation

The displacement between the onset of plastic deformation and the maximum load shall be determined from the load-displacement chart. Uniform elongation shall be expressed as a percentage and obtained by dividing this displacement by the gage length and multiplying by 100.

7.5 Reduction of Area

7.5.1 The change in specimen diameter due to testing shall be determined by fitting together the broken ends of the specimen and measuring the diameter at the smallest section. This measurement shall be made at three different angular orientations and the mean of the three taken as a valid measurement. The value shall then be used to determine a cross-sectional area that shall be subtracted from the original cross-sectional area to obtain the decrease in cross-sectional area due to testing.

7.5.2 Reduction in area shall be expressed as the percentage decrease in cross-sectional area and obtained by dividing the decrease in cross-sectional area by the original cross-sectional area and multiplying by 100.

8. Test Record

8.1 The test record shall contain the following results or information:

(a) Project title and account number
(b) Test machine identifier
(c) Date of test
(d) Operator
(e) Specimen identifier
(f) Specimen dimensions
(g) Gage length
(h) Test temperature
(i) Speed of testing
(j) Specimen dimensions after test
(k) Change in gage length
(l) 0.2% offset yield strength
(m) Tensile strength
(n) Total elongation
(o) Uniform elongation
(p) Reduction in area

8.2 The test report shall include any autographic load-displacement charts obtained in the test.

8.3 The designation of the procedure followed, including revision identification, shall be recorded on the test record and the test record shall be countersigned by the LRC Project Leader.

APPENDIX F

LRC-TP-80 (1/26/82)
Charpy Impact Testing of Metallic Materials

1. Introduction

This Technical Procedure describes a method for notched-bar impact testing of metallic materials by the Charpy apparatus and conforms to ASTM E23-81, "Standard Methods for Notched Bar Impact Testing of Metallic Materials."

2. Operator Qualification

Charpy impact test Operators shall be qualified by training and experience and shall have demonstrated competence to perform the tests in accordance with this Procedure to the satisfaction of the LRC Project Leader.

3. Specimen

3.1 The specimen shall be a Charpy impact test specimen, Type A (V-notch), as shown in ASTM E23-81, Figure 6.

3.2 Subsize specimens may be used if so designated by the LRC Project Leader. If subsize specimens are used, specimen size and the justification for such use shall be noted on the test report.

4. Equipment

4.1 Testing Machine

The Charpy impact test machine shall be a pendulum type of rigid construction and of capacity at least 125% of that required to break each specimen. The machine shall be rigidly mounted to either a concrete floor not less than 6 inches thick or a base of a weight at least 40 times that of the pendulum. The machine shall conform to ASTM E23-81, Section 4.

4.2 Self-Centering Tongs

A set of tongs, as shown in ASTM E23-81, Figure 14, shall be used to center the specimens within the testing machine's anvils.

4.3 Instrumented Data Acquisition

The impact machine shall be equipped with a "Dynatup" instrumented tup, signal conditioning unit, and data storage unit suitable for recording both load and energy versus time information.

4.4 Temperature Conditioning

Heating and cooling chambers shall be of the liquid immersion type. The bath temperature measuring device shall be placed near the center of a group of immersed specimens. The fluid shall be agitated continuously. The heating and cooling chambers shall have a grid raised at least 1 inch from the bottom to provide a specimen support. The fluid shall be of sufficient depth so that the specimens when immersed shall be covered by the liquid by at least 1 inch.

Desired temperature shall be maintained within ±2F (±1C) and measured with mercury-in-glass thermometers conforming to ASTM specification E1.

5. Inspections and Calibrations

5.1 Impact Machine

5.1.1 Initial Inspection

At installation, the test machine shall be inspected to assure conformity with the requirements of ASTM E23-81.

5.1.2 Annual Qualification

The impact tester shall be qualified by testing standardized specimens and obtaining evaluation from the Army Materials and Mechanics Research Center (Watertown, Massachusetts) at least annually. If the machine is moved, repaired, adjusted, or if there is any reason to doubt the accuracy of the results, or if the pendulum is stopped by a specimen during test, or if the test value obtained exceeds 80% of the test machine's capacity, then the tester shall be requalified without regard to the time interval.

5.1.3 Daily Check

(a) At least once daily, the machine shall be checked by a free swing of the pendulum. With the indicator at the maximum energy position, a free swing of the pendulum shall indicate zero energy.

(b) At the discretion of the LRC Project Leader, an aluminum calibration specimen shall be tested at room temperature in a manner otherwise identical to subsequent tests.

5.2 Instrumented System

The data storage unit(s) of the instrumented impact system shall be calibrated at least annually against standards traceable to the National Bureau of Standards (NBS). The system as a whole shall be checked daily by comparison of an energy value recorded by the instrumented system with that indicated on the impact tester.

5.3 Temperature Measurement

Thermometers used for temperature measurement shall be calibrated against NBS traceable standards within 3 months before the test.

5.4 Lateral Expansion Measurement

The dial indicator used for the measurement of lateral expansion shall be calibrated at least annually against NBS traceable standards.

5.5 Percent Shear Fracture Determination

If a dial caliper is used in the determination of percent shear fracture, it shall be calibrated at least annually against NBS traceable standards.

6. Test Procedure

6.1 Test Redundancy

The number of "identical" specimens to be tested at each temperature shall be as determined by the LRC Project Leader.

6.2 Specimen Heating and Cooling

Nominal test temperatures shall be designated by the LRC Project Leader. Specimens shall remain immersed in the liquid medium for not less than 10 minutes.

6.3 Specimen Placement

Self-centering tongs shall be used for alignment of the specimen within the machine anvils. The specimen-gripping portion of the tongs shall be cooled or heated with the specimens.

6.4 Machine Preparation

The pendulum shall be placed in its latched position. The energy indicator shall be set at its maximum energy position. The "Dynatup" instrumented system and the computer data acquisition system shall be prepared to receive data.

6.5 Test Operation

6.5.1 The specimen shall be removed from the immersion bath with the tongs and centered between the machine's anvils. The pendulum shall then be released from its latched position. This entire operation shall be completed within 5 seconds. The energy valve shall be read from the indicator prior to locking the pendulum for the next test.

6.5.2 If the specimen fails to break, the test shall be terminated for that specimen. The LRC Project Leader shall be immediately notified. The fact shall be recorded indicating whether the break occurred through extreme ductility or lack of sufficient energy in the blow. The results of such tests shall not be used for material evaluation.

6.5.3 If the specimen jams in the machine, the test should be terminated for that specimen. The LRC Project Leader shall be immediately notified. The results of that test shall be disregarded and the machine shall be checked for damage or maladjustment and the requirements of Section 5.1.2 shall be followed.

6.5.4 After testing, specimens shall be carefully removed from the tester or specimen catcher and maintained as specimen pairs by placing in plastic bags, by taping together, or as otherwise convenient in accordance with requirements established by the LRC Project Leader.

7. Procedures for Obtaining Test Results

7.1 Impact Energy

Charpy Impact Energy shall be read to the nearest integer on the tester's energy indicator. The maximum energy signal on the oscilloscope ($E_a$max) shall be read to the nearest determinable value.

7.2 Lateral Expansion

Lateral expansion shall be determined in accordance with the following procedure.

7.2.1 Measurements shall be taken on a gage consisting of a dial indicator rigidly mounted to a fixture. The fixture shall provide reference supports for locating broken specimen with respect to the dial indicator. The dial indicator shall be equipped with a flat anvil to provide proper contact with the specimen. This gage shall conform in principle to ASTM E23-81, Figures 17 and 18.

7.2.2 The broken specimen halves shall be retrieved and paired. The sides perpendicular to the notch shall be visually inspected to ensure that they are free from burrs (as would be formed during impact testing). If such burrs are present, they shall be removed (as by rubbing on emery cloth), making sure that the protrusions to be measured are not disturbed. The fracture surface shall be visually examined to ascertain that the protrusions have not been damaged as by contacting the anvil or machine mounting surface. Damaged specimens shall not be measured for lateral expansion except if decided otherwise by the Project Leader.

7.2.3 The halves shall be placed together so that the compression sides are facing one another. One half shall then be taken and pressed firmly against the reference supports with the protrusion against the gage anvil. The reading shall be noted and the measurement repeated with the other broken half, ensuring that the same side of the specimen is measured. The larger of the two readings shall be taken as the expansion of that side of the specimen. This procedure shall then be repeated to measure the protrusion on the opposite side. The larger values for each of the two sides shall be added together and this sum, expressed in mils, shall be recorded as the lateral expansion for that specimen.

7.3 Fracture Appearance

Percentage of shear fracture shall be determined in accordance with the methods of 7.3.1 or 7.3.2, below. The LRC Project Leader shall select the method to be followed.

7.3.1 Measurement Method -- The length and width of the cleavage portion of the fracture surface shall be directly measured with a dial caliper and the percentage of shear fracture determined therefrom. "Length" and "width" are defined in ASTM E23-81, Figure 14. Determination of percentage values shall be by use of ASTM E23-81, Table 1 or Table 2.

7.3.2 Comparison Method -- The appearance of the fracture surface shall be visually compared with those in ASTM E23-81, Figure 15, and the values obtained therefrom shall be taken as the percentage of shear fracture.

8. Test Record

8.1 The test record shall contain the following results or information in columnar form:

(a) Specimen identifier

(b) Test temperature, F

(c) Impact energy, dial, in ft-lbs

(d) Impact energy, Dynatup, ($E_a$max), in ft-lbs

(e) Lateral expansion, in mils

(f) Percentage of shear fracture

(g) Oscilloscope readings

(i) Load, in lbs/div

(ii) Sweep speed, in msec/div

8.2 The test record shall also contain the following information:

(a) Project title and account number

(b) Specimen size and justification for use if subsize specimens were used

(c) Date of each test

(d) Operator for each test

8.3 The designation of the procedure followed, including revision identification, shall be recorded on the test record and the test record shall be countersigned by the LRC Project Leader.

8. REFERENCES

1. J. A. Davidson, J. H. Phillips, and S. E. Yanichko, Virginia Electric & Power Company North Anna Unit 2 Reactor Vessel Radiation Program, WCAP-8772, Westinghouse, Pittsburgh, Pennsylvania, November 1976.

2. DOT 3.5 -- Two-Dimensional Discrete Ordinates Radiation Transport Code, (CCC-276), WANL-TME-1982, Oak Ridge National Laboratory, Oak Ridge Tennessee, December 1969.

3. CASK -- 40-Group Coupled Neutron and Gamma-Ray Cross Section Data, RSIC-DLC-23, Radiation Shielding Information Center, Oak Ridge Tennesse, March 1975.

4. H. S. Palme and H. W. Behnke, Methods of Compliance With Fracture Toughness and Operational Requirements of Appendix G to 10 CFR 50, BAW-10046A, Babcock & Wilcox, Lynchburg, Virginia, July 1977.